Advances in Water Resources 216 (2026) 105432

Contents lists available at ScienceDirect

Advances in Water Resources

journal homepage: www.elsevier.com/locate/advwatres

Stochastic Hydrology Reveals the Controls of Forest Harvesting - Peakflow Causal Relations in Snow-Transient Environment

WeiTao Nick Rong *, Kyle S. Bishop, Younes Alila

Forest Resources Management, Faculty of Forestry & Environmental Stewardship (FES), University of British Columbia, 2424 Main Mall, Vancouver, British Columbia, V6T 1Z4, Canada

ARTICLE INFO

Dataset link: Hydrological and GIS data from H.J. Andrews Experimental Forest LTER Data Bank (Reference data)

Keywords:
Hydrological causality
Probabilistic understanding
Peak discharges
Stochastic hydrology
Forest hydrology
Snow-transient environments

ABSTRACT

Understanding and predicting how forest harvesting alters peakflows is essential for managing downstream risk, as changes in forest cover can intensify extreme events, affecting water quality, infrastructure, ecosystems, and public safety. In light of this, the drivers of snow-transient peakflows must be better characterized. This study presents a probabilistic meta-analysis using nine pairs of control-treatment watersheds in the snow-transient environments of the Pacific Northwest to show how harvesting, in some cases, can dramatically increase the magnitude and frequency of not only the small ($\leq$ 10-yr) but also large (>10-yr) peakflows. Under certain hydro-climate and watershed conditions, the effects on the magnitude and frequency of peakflows increase with increasing event size. Subdued landscapes and drier and warmer environments have emerged as effective indicators of conditions where the peakflow regime is most sensitive to harvesting practices. This probabilistic framework can yield predictive outcomes that differ from long-held deterministic expectations in forest hydrology, particularly regarding how harvesting affects large peakflows. To draw a comparison with the development of statistical mechanics in thermodynamics, it appears the introduction of probability in forest hydrology, too, could suddenly reverse the prevailing perspective of the old deterministic framework and stimulate a paradigm-induced gestalt switch in the physical understanding and prediction of forest harvesting effects on peakflows.

1. Introduction

Understanding and predicting how forest harvesting affects floods in large watersheds, and peakflows in smaller watersheds, informs forest management policy and helps minimize consequences to downstream values. Given our ability to influence hydrologic response through forest harvesting and/or climate change, the timing, magnitude, and frequency of extreme peakflows are impacted, departing from natural conditions (Blum et al., 2020). An increased risk of peakflows can degrade water quality (Alexander et al., 2007), damage infrastructure (Kumar et al., 2021), disrupt fluvial ecosystems (Talbot et al., 2018), harm fish in the stream (Naman et al., 2024), heighten drought risk in subsequent seasons (Hammond et al., 2025), and endanger human lives (Ashley & Ashley, 2008). Rain-on-Snow (ROS) events have led to costly flooding disasters such as the 2021 atmospheric river event in southwestern British Columbia (Gillett et al., 2022). Forest cover changes through harvesting and wildfires may have played an increased role in this event (Hancock & Wlodarczyk, 2025), especially with concerns of shifting winter precipitation to predominantly rainfall with a changing climate. This underscores the need to better understand the physical drivers of peakflows and how they are influenced by forest disturbance in ROS environments.

1.1. Towards a Contextual and Causal Understanding of Peakflows

Forest harvesting effects on peakflows have been traditionally assessed using a deterministic framework, with limited application of a probabilistic framework. The deterministic framework quantifies changes in peakflow magnitudes through pre- and post-harvest comparison under equal storm input in the rain environment and equal freshet season in the snow environment. However, by design, this framework does not account for the frequency with which such events occur and therefore leads to a non-causal experimental design (Pham & Alila, 2024). By contrast, the probabilistic framework evaluates the effects of forest disturbance on both the magnitude and frequency of peakflows simultaneously, enabling an experimental design that is

* Corresponding author.
E-mail address: nick.rong@alumni.ubc.ca (W.N. Rong).

https://doi.org/10.1016/j.advwatres.2026.105432
Received 13 April 2026; Received in revised form 18 July 2026; Accepted 18 July 2026
Available online 18 July 2026

causal in nature (Kaluarachchi & Alila, 2025; Pham & Alila, 2024).

If a probabilistic framework is required to predict forest harvesting effects on peakflows and capture its causal relationship, then interpretations made through physical understanding should also stem from the same framework. The flood frequency curve (FFC) "represents one of the most comprehensive and compact descriptions of a catchment's storm response" because it captures the dynamic interplay between runoff generation mechanisms and the physical characteristics of the watershed and climate (Robinson & Sivapalan, 1997). Although relatively new to forest hydrology, a probabilistic approach to understanding the watershed response is well established in the broader literature, where it is referred to as stochastic hydrology (Blöschl & Sivapalan, 1997; Merz & Blöschl, 2009) and was pioneered by Eagleson (1972), Klemeš (1978), and Yevjevich (1974). Current understanding of the magnitude-frequency relationship is grounded in over half a century of literature that interprets the environmental controls of floods using a probabilistic framework (Pham & Alila, 2024, and references therein). Through a probabilistic framework, the location, scale, and shape parameters of the peakflow or flood frequency curve reflect interactions between watershed physiography and climate, resulting in changes to peakflows following forest harvesting. Such parameters are functions of the mean, variability, and skewness of the time series of peakflows. Forest-harvesting-induced changes to FFC parameters arise from altered runoff mechanisms, which in turn are highly dependent on the physical characteristics of the watershed and climate (Sivapalan et al., 1987). Depending on whether Water Available for Runoff (WAR) has increased, runoff is synchronized (i.e., delivered more efficiently to the streams) and/or desynchronized (i.e., efficiency is impeded), the mean, variability, and/or skewness can increase, decrease, or remain unchanged (Figure 1). Probabilistic forest hydrology

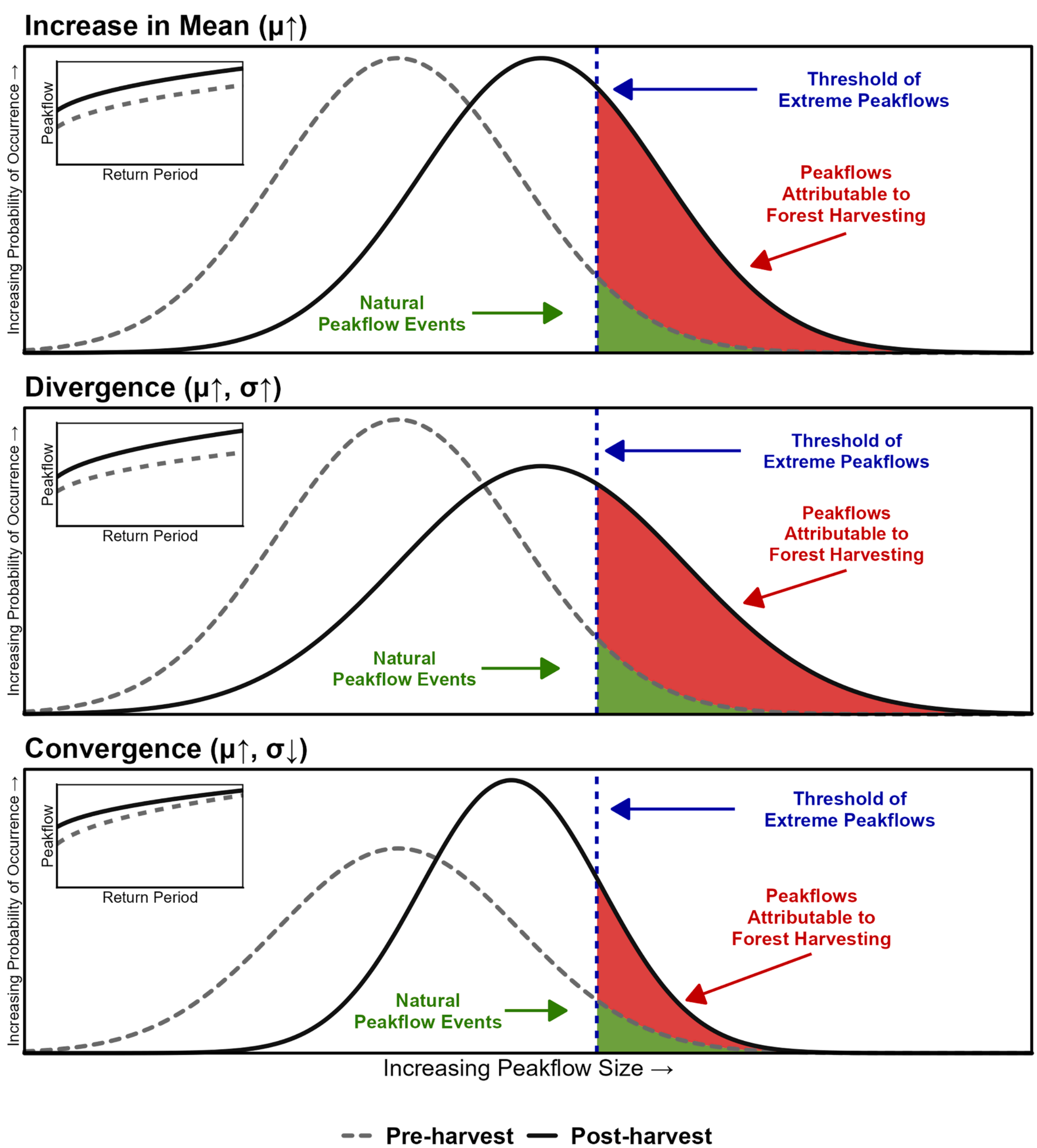

Figure 1. Conceptual diagram illustrating how forest harvesting alters the mean and variance of the natural peakflow frequency distribution, depending on a watershed's physical characteristics and climate. Top panel: parallel FFCs indicating an increase in mean only with increases in peakflow magnitude and frequency. Middle panel: diverging FFCs indicating an increase in mean and variance with larger increases in magnitude and frequency. Bottom panel: converging FFCs indicating an increase in mean and a decrease in variance, resulting in smaller increases in magnitude and frequency. Skewness is also influenced, but has been left out of this figure for simplicity.

studies invoking stochastic understanding to explain the causes of FFC parameter shifts continue to grow as a body of literature in the rain and snow environments (Green & Alila, 2012; Johnson & Alila, 2023; Kaluarachchi & Alila, 2026; Pearson-Atkins et al., 2026; Pham et al., 2025; Pham & Alila, 2024).

1.2. Snow-Transient Environments: Beyond Stand-level

ROS environments express characteristics of both rain- and snow-dominated watersheds, yet far more research has addressed stand-level snow mass and energy balance than watershed-level ROS dynamics (Berris & Harr, 1987; Harr et al., 1989; Storck et al., 2002); as Jennings and Jones (2015) note, decades of rain-on-snow research have yielded limited insight into snowpack dynamics during storms. Forested stands accumulate less snow than open sites because of canopy interception, sublimation (Lundberg et al., 1998), and enhanced longwave input (the "radiative paradox"; Sicart et al. (2004)), and where winter temperatures hover near 0°C, canopy-intercepted snow, meltwater drip, and fog drip add energy that further reduces sub-canopy snow (Beaudry, 1984; Berris & Harr, 1987). Although fog interception can add 20–30% more precipitation beneath the canopy (Harr, 1982; Ingwersen, 1985) and up to 72% of intercepted snow can be released as meltwater drip (Storck et al., 2002), the direct influence of fog and meltwater drip on snowpack energy balance remains largely uninvestigated. During events, wind and turbulence are the dominant melt-energy source, with advective energy from rain secondary (Harr & Coffin, 1992), and the resulting activation time of the snowpack depends most strongly on elevation.

Elevation, however, interacts nonlinearly with aspect and vegetation. Working within a probabilistic framework, Brunengo (2012) showed that, although ROS occurs across a wide elevation range, there is a narrow peak-ROS elevation band where water available for runoff (WAR) most often exceeds precipitation: below it, thin, patchy snowpacks contribute little to WAR, whereas above it, thick, cold snowpacks retain rainfall. An earlier effort to relate basin elevation to peak-ROS behaviour (Christner & Harr, 1982) found the largest specific 10-year peakflows near a mean elevation of 850 m but, given the scatter, drew no inferential conclusions. Consistent with Brunengo, the during-event modelling of Garvelmann et al. (2015) showed that, in watersheds with large elevation gradients, higher-elevation snowpacks contribute to WAR later than lower-elevation ones, so small elevation differences strongly affect the lag between rainfall onset and snowpack runoff contribution - making a snowpack's watershed-scale role elevation-dependent, in a manner analogous to the Variable Source Area concept (Hewlett & Hibbert, 1967), an analogy not previously invoked in ROS hydrology.

Forest roads extend the natural drainage network and raise drainage efficiency by adding impervious area, intercepting surface and subsurface flow, and re-routing runoff through ditches connected to streams and gullies, so that, on routing efficiency alone, roads can increase synchronization and peak discharge at the outlet (Jones, 2000; Jones & Grant, 1996). These controls interact stochastically with aspect, slope, watershed shape, drainage-network geometry, storage, and catchment size to promote synchronization or desynchronization of runoff delivery to the channel (Figure 1); a probabilistic framework, supported by stochastic understanding, is therefore needed to interpret their combined effect on the peakflow magnitude-frequency relation. To our knowledge, no previous study has applied stochastic understanding and prediction to the ROS environment of the Pacific Northwest, underscoring the need for watershed-level probabilistic analyses.

1.3. Objectives and Hypotheses

This study applies a probabilistic framework to nine pairs of control-treatment watersheds, using long-term datasets from the snow-transient environment (where winter air temperatures hover near 0°C and rain-on-snow events are central to peakflow generation) in Oregon (USA) to evaluate the effects of varied forest harvesting practices. The large observed flow dataset enables a detailed examination of harvesting impacts across a range of watershed conditions. Furthermore, the use of a meta-analysis approach is necessary in understanding and distinguishing the multiple, chancy drivers affecting the causal relationship between forest harvesting and peakflows.

The primary objective of this study is to advance the stochastic understanding of forest hydrology in ROS environments. Outside forest hydrology, it is a long-recognized principle that extremes are highly sensitive to even small changes in the mean and/or variability, resulting in surprisingly large changes in the frequency of extreme events (Katz, 1993; Katz & Brown, 1992). Accordingly, and as imposed by the statistics of extremes, this study aims to understand and predict how forest harvesting-induced changes in the mean and variability of peakflows influence the magnitude and frequency of extreme peakflows at the upper tail of the FFC. The second objective of this study is to investigate how forest harvesting-induced changes in WAR and in the efficiency of runoff delivery to the channels (i.e., synchronization/desynchronization), influence the mean and variability of peakflows in the ROS environment, as previously demonstrated by Green and Alila (2012) and Schnorbus and Alila (2013, 2004) in snowmelt-dominated environments and by Pham et al. (2025) in rain environments. The third objective of this study is to assess how watershed-scale physiography and climate govern peakflow sensitivity to forest harvesting in snow-transient environments.

We aim at testing the following hypotheses:

H1. Watershed elevation range controls the extent of synchronization of runoff generation through snow mass and energy balance; higher synchronization effects lead to a larger increase in the mean and variability of the peakflows following harvesting.
H2. Road network increases the routing efficiency of the watershed and the resulting increased runoff, reduced response timing, and enhanced synchronization lead to higher means and higher variability of peakflows.
H3. Tree removal suppresses fog interception in certain humid environments, which in turn increases the mean and variability of the peakflows as a consequence of an increase in baseflow and an intensification of the ROS phenomenon; making the peakflow regime of such humid environments with the presence of fog interception one of the most sensitive to forest harvesting.
H4. In the Snow-Transient Zone (STZ) of the Pacific Northwest (STZ is roughly defined as elevation 450 ~ 1100 m above sea level), where snow is more important in peakflow generation, peakflows in watersheds with drier climates are more sensitive to tree removal as manifested by larger increases in the mean and variability of peakflows.
H5. The magnitude of infrequent peakflows (defined as events with a return period larger than 10 years) can be substantially affected by tree removal and road building, as a direct consequence of the increase in the mean and/or variability of peakflows articulated in hypotheses 1 through 4 above.
H6. Within the range of observed post-harvest peakflows (17 to 50 years), tree removal and forest road effects on the magnitude and frequency of peakflows can increase unchecked with event size, i.e. with no apparent 'no-effect' threshold for the influence of forest harvesting on peakflow response. This again is a direct consequence of such an increase in the mean and/or variability of peakflows articulated in hypotheses 1 through 4 above.

Given these six hypotheses, the Discussion section will incorporate the use of stochastic understanding to provide physically based explanations for observed changes in FFC parameters induced by forest harvesting.

2. Materials and Methods

2.1. Study Sites

This study uses nine pairs of control-treatment watersheds from three study sites: Coyote Creek (CC), Fox Creek (FOX), and H.J. Andrews Experimental Forest (HJA). In Coyote Creek, the treatment watersheds are CC1, CC2, and CC3; all with CC4 as control. In Fox Creek, FOX1 and FOX3 are treated and both use FOX2 as a control. In H.J. Andrews, treatment watersheds HJA1 and HJA3 use HJA2 as control, HJA6 uses HJA8 as control, and HJA10 uses HJA9 as control. Although all three sites are located within the state of Oregon (U.S.A.), and are subject to similar larger-scale climate patterns, the local climate and vegetation conditions at the three study sites are hydrologically distinctive. Fox Creek is at the northern end of Oregon, close to Washington, and Coyote Creek is in the southern part of Oregon, closer to California; H.J. Andrews is located in the middle, about 130 to 150 km from the other two sites (Figure 2). Detailed environmental conditions of the three sites are discussed below.

2.1.1. Climate

All three sites are characterized by a distinctive dry, hot summer and

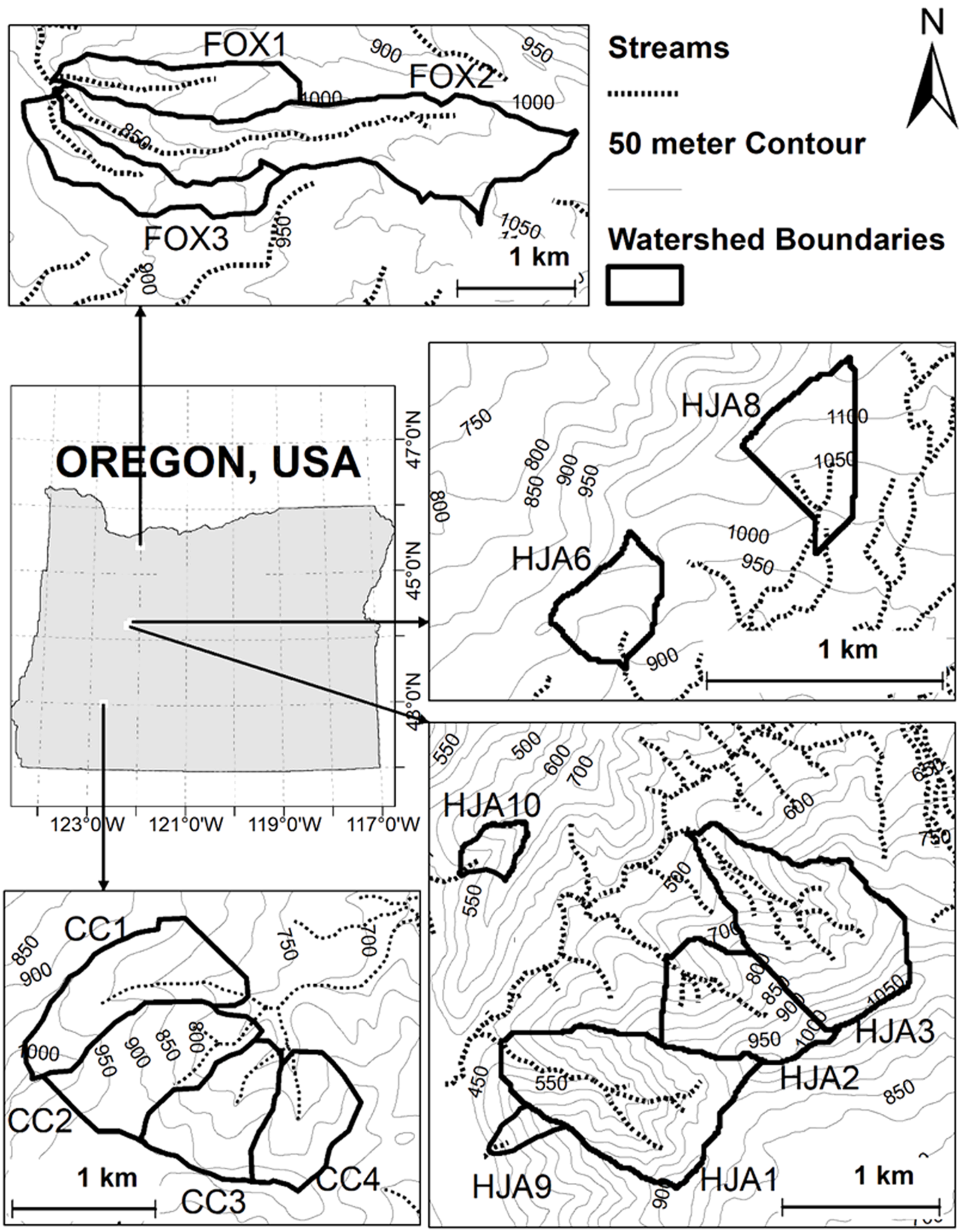

Figure 2. Locations of the three study sites in the state of Oregon and the configurations of watersheds within each site.

wet, cool winter. The long-term climate normal statistics (1961-1990) of the three sites, with output from ClimateWNA (v.5.3, Wang et al. 2012) show that Coyote Creek, being in the southern part of Oregon, is warmer and receives significantly less precipitation than the other two sites all year round (Figure 3). The average annual precipitation is about 2600 mm, 2300 mm, and 1100 mm for Fox Creek, H.J. Andrews, and Coyote Creek, respectively. Fox Creek and H.J. Andrews receive comparable amounts of precipitation in the fall and winter, but Fox Creek receives noticeably more precipitation than H.J. Andrews in the spring and summer (Figure 3). Also, a stand-level water balance experiment at Fox Creek found that the area beneath the forest canopy receives 20∼30% more water annually due to the fog interception phenomenon as compared with the nearby open area (Harr, 1982). In winter (December to February), Fox Creek and H.J. Andrews receive comparable monthly precipitation (∼340 mm) while Coyote Creek receives far less (∼144 mm), and Coyote Creek is roughly 2-5°C warmer than the other two sites year-round (Figure 3). Even with the same precipitation amount, the warmer temperature in Coyote Creek likely contributes to the drier conditions via stronger evaporation and sublimation. Detailed annual water balance calculations have demonstrated that Coyote Creek has a lower net moisture input than the other two sites (Jones, 2000).

Precipitation and temperature normally change with elevation. Such variation is reasonably controlled by the experimental design of a paired watershed study (control and treatment watersheds are adjacent and have similar elevation ranges). However, elevation control on precipitation and temperature is potentially a confounding factor in inter-pair comparisons of the sensitivity of peakflow response to treatment if the two pairs are sitting at different elevations. Unlike Fox Creek and Coyote Creek where there is only one control watershed, the H.J. Andrews site has three control watersheds: HJA2 (outlet at 545 m), HJA8 (outlet at 962 m), and HJA9 (outlet at 426 m). The pair of HJA6/HJA8 is at a higher altitude than the other three pairs of HJA watersheds. Using ClimateWNA (v.5.3) normals (1961-1990) for H.J. Andrews, winter precipitation rises from ∼287 mm at 500 m to ∼354 mm at 1000 m (∼0.13 mm/m), and air temperature falls with elevation at about 2.5-6.3°C/km (Rosentrater, 1997). Since temperature and precipitation are affected by factors other than elevation, the actual lapse rates could vary significantly from event to event.

Controlled by different combinations of local climate, elevation and aspect, snow accumulation and melt are different between watershed pairs. Being higher in elevation, with their outlets above 800 m, the two pairs of watersheds in Fox Creek and HJA6/HJA8 have snow depths sometimes exceeding 1.5 m and persisting for up to half a year (Harr, 1982). Although watersheds in Coyote Creek have an elevation range similar to those of watersheds in Fox Creek and HJA6/HJA8, the snowpack in Coyote Creek normally melts away within 1-2 weeks after snowfall due to the drier and warmer local climate (Harr et al., 1979). In H.J. Andrews, snowpack development in HJA10/HJA9 is weak and normally melts away within 1-2 days after the snowfall due to their lower elevation (outlet at around 460 m) (Harr & McCorison, 1979). With a difference in melting time from days to half a year between HJA10/HJA9 and HJA6/HJA8, snowpack within the STZ exhibited high sensitivity to small elevation changes. Watersheds HJA1, HJA2, and HJA3 have much larger elevation ranges than other watersheds in this study (Table 1) and almost completely cover the entire elevation range of the STZ, which is roughly around 450 ∼ 1100 m in this region of the Pacific Northwest. The outlet elevations of HJA1 and HJA3 are similar to the 460 m outlet elevation of HJA9 and HJA10 and the upper elevations are all above 1000 m, like the higher-elevation watersheds in Coyote and HJA6.

2.1.2. *Rocks and Soils*

Overland runoff rarely occurs in the western Cascadia range of Oregon due to high soil infiltration rates which exceed 2000 mm/h (Jones, 2000). Prolonged water input increases the pore-water pressure between soil particles and therefore the risk of landslide and mass movement, especially on slopes with a poorly developed external drainage pattern (Harr et al., 1979). Among the watersheds in this study, average slope gradient increases from watersheds in Fox Creek (<10%), to watersheds in Coyote Creek and HJA6/HJA8 (30%), to HJA1/HJA2/HJA3/HJA9/HJA10 (>60%) (Jones, 2000). Site-consistent data on soil depth and storage capacity are not available across the nine watersheds; however, the very high infiltration rates and near-absence of infiltration-excess overland flow throughout the study sites suggest that differences in soil storage are unlikely to be the primary control on the between-site differences in peakflow sensitivity to harvesting, which we instead attribute to the spatial synchronization of water available for runoff (Section 4.1).

2.1.3. *Vegetation and Treatments*

Vegetation at these three sites in each case was dominated by high Leaf Area Index (LAI) old-growth coniferous trees before any forest

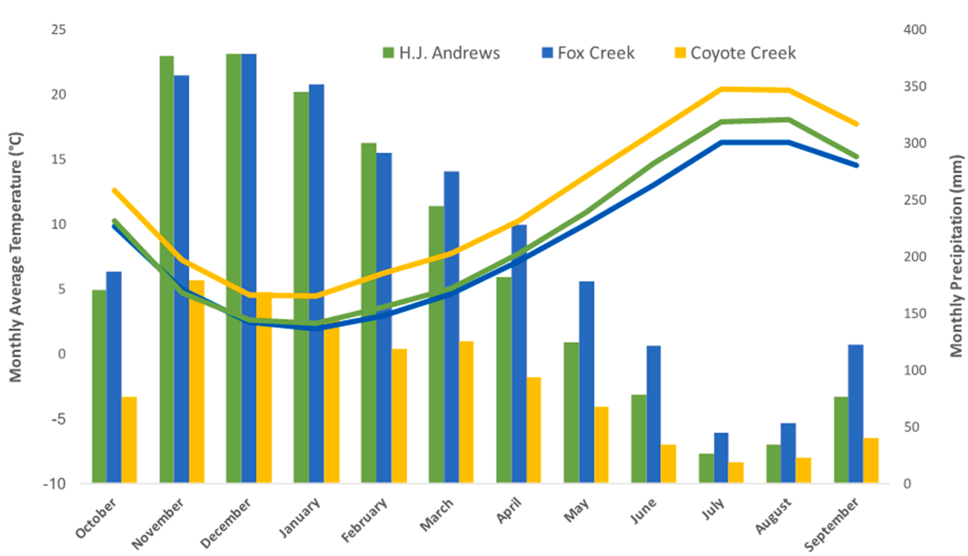

Figure 3. Long-term climate normals (1961-1990) of H.J. Andrews (green), Fox Creek (blue) and Coyote Creek (yellow). Average air temperatures (°C) are shown in solid lines and monthly accumulated precipitation measures (mm) are shown in bars; both follow the color scheme of the three sites described above. The data are generated using PRISM long-term climate statistics (PRISM Climate Group, 2004) and downscaled by the ClimateWNA mode (Wang et al., 2012) with an assumed 900 m elevation.

Table 1
Watershed characteristics and history of harvesting practices. Harvest methods provided by (Harr, 1983, 1980; Harr et al., 1979; Perry & Jones, 2017).

Sites	Pair (Treatment-Control)	Treatment			Available Record (Water Year)		Size (km^2)	Elevation (m)		Elevation Range (m)	Aspect (degree)
		Harvest (%)	Harvest methods	Road (km/km^2)	Pre-treatment period	Post-treatment period		Lower Bound	Upper Bound		
Coyote	CC1-CC4	50	50% tractor	2.2	WY63-70	WY72-81 & WY00-13	0.69	750	1065	315	45-90 NE-E
Coyote	CC2-CC4	30	16% high-lead cable yarding, 14% tractor	4.1	WY63-70	WY72-81 & WY00-13	0.68	760	1020	260	45 NE
Coyote	CC3-CC4	100	77% high-lead cable yarding, 23% tractor	3.2	WY63-70	WY72-81 & WY00-13	0.5	730	960	230	0-45 N-NE
Fox	FOX1-FOX2	25	25% high-lead cable yarding	2.1	WY58-64	WY70-87	0.59	840	925	85	270 W
Fox	FOX3-FOX2	25	19% high-lead cable yarding, 6% tractor	1.3	WY58-64	WY70-87	0.71	840	950	110	315 NW
HJA	HJA1-HJA2	100	100% skyline yarding	0	WY56-61	WY67-14	0.96	439	1027	588	286 W-NW
HJA	HJA3-HJA2	25	25% high-lead cable yarding	2.7	WY56-58	WY64-14	1.01	471	1080	609	313 NW
HJA	HJA6-HJA8	100	90% high-lead cable yarding, 10% tractor	4.6	WY63-73	WY75-14	0.13	878	1029	151	165 S-SE
HJA	HJA10-HJA9	100	40% skyline yarding, 60% tractor	0	WY68-74	WY76-14	0.1	461	679	218	250 W-SW

harvesting activities. Common species include: Douglas fir (*Pseudotsuga menziesii*), western hemlock (*Tsuga heterophylla*), western red cedar (*Thuja plicata*), mountain hemlock (*Tsuga mertensiana*), and Pacific silver fir (*Abies amabilis*) (Jones, 2000). Treatment (harvesting extent and method, and road building) varies among watersheds. In terms of harvesting, rate increases from 25%-35% patch-cut in FOX1, FOX3, CC2, and HJA3, to 50% selection cut in CC1, to 100% clearcut in CC3, HJA1, HJA6, and HJA10 (Table 1). All treated watersheds except HJA1 and HJA10 have forest roads, with road densities ranging from 1.3 to 4.6 km/km^2.

2.2. Data Collection and Analysis

The long-term normal climate statistics came from the PRISM data (PRISM Climate Group, 2004) and were extracted and spatially disaggregated by the ClimateWNA software (Wang et al., 2012). Discharge data were obtained from the H.J. Andrews Experimental Forest data bank (part of the U.S. LTER network); calibration periods range from two to ten years. The post-treatment period also varies among studied watersheds, with watersheds in H.J. Andrews having a longer post-treatment record of 38 to 50 years and watersheds in Fox Creek and Coyote Creek having a shorter post-treatment record of 17 to 22 years. The Coyote Creek post-treatment record comprises two segments (1972-1981 and 2000-2013) owing to a monitoring interruption; under the time-recovery linearity assumption described below, the effect of this gap is expected to be small.

The selection of peakflows from the long-term flow measurements has been done according to the method described in Jones (2000), which involves two steps. First, the hourly peak discharge data in each watershed are filtered with a watershed-specific minimal threshold which is set to produce an initial dataset of 10-15 events per year on average. Second, the selected peaks in the treated and control watersheds are paired. Peakflows in the treated and control watersheds are paired when occurring within 12 hours of each other. The resulting final dataset contains 9-12 matched events per year on average in each pair of watersheds. Occasional missing records (gauge malfunction, etc.) were gap-filled with estimates from the stream-gauge manager; because such estimates can be unreliable for extreme events (USDA-NRCS, 2007), a small percentage of peaks flagged as estimated were excluded to reduce uncertainty in the frequency analysis (Beschta et al., 2000).

The frequency analysis of observed (representing post-harvest) and expected (representing pre-harvest) peakflows is done according to the method described in Alila et al. (2009) and Green and Alila (2012), which involves three major steps: estimation of the expected discharge, peakflow frequency analysis, and adjustment for non-stationarity caused by forest regrowth. Before treatment is applied (the calibration period), the treated and control watersheds have similar conditions and therefore their responses to the same storm input are highly correlated. A linear regression developed from the selected peaks in the calibration period is used to predict the expected peakflow magnitudes of a treated watershed in the post-treatment period as if the treatment was never applied:

$$\widehat{Y}_i = b_0 + b_1 X_i, \quad (1)$$

where $\widehat{Y}_i$ is the expected peakflow in the treatment watershed and X_i is the peakflow in the control watershed. The use of linear regression in developing the calibration equation is scientifically defensible as long as the conditions of the two watersheds as well as meteorological forcings are tightly controlled, which is the case under pre-harvest conditions (Green & Alila, 2012). The goodness of fit of these calibration regressions for the nine watershed pairs is summarized in Table S1. However, linear regression should not be used in the post-treatment period because the pre-event and event conditions between the two watersheds (for example, AMC, snow, and meteorology) are no longer the same. It is well known in the modelling community that offsets in the initial conditions of complex systems would produce drastically different behaviors and responses even if the subsequent forcings are identical (see literature related to chaos theory in hydrology such as Sivakumar (2017)).

For peakflow frequency analysis, this study follows the Partial Duration Series (PDS) frequency analysis described in Alila et al. (2009). The peakflow (Q_p) of the treated watershed in the post-treatment period is the *observed peakflow* with treatment effects. With a sample size of n, the observed peakflows Y_i (i.e. chronological event $i = 1, 2, 3, \ldots, n$) are then ranked from largest to smallest and the exceedance probability $1-p$

of the j^{th} largest event Y_j is estimated by the approximately quantile-unbiased Cunnane plotting position (Stedinger et al., 1993):

$$1 - G_Y[Y_j] = \frac{j - 0.40}{n + 0.20} \tag{2}$$

where G_Y is the cumulative distribution function (CDF) of Y. Because there are more than one independent events per year in the PDS, the estimation of the return periods considers the average arrival rate λ (the average number of peakflow events per year above the selected threshold). Following the procedures outlined in Section 18.6 of the *Handbook of Hydrology* (Stedinger et al., 1993, Editor D. Maidment), the annual return period T_a is calculated as:

$$T_a = \frac{1}{1 - \exp(-\lambda * [1 - G_Y])} \tag{3}$$

and the PDS return period (T_p) is calculated as:

$$T_p = \frac{1}{\lambda * [1 - G_Y]} \tag{4}$$

and the two return periods T_p and T_a become essentially the same for infrequent events (when $T_a > 10$ year) (Langbein, 1949). The frequency curve of the observed peakflow is then plotted as Historic Probability of Non-exceedance (p) and PDS return period (T_p) versus peakflow magnitude (Q_p).

The same ranking and return period calculation procedure is then applied to produce a series of ranked expected peakflows $\widehat{Y}_j$. To correct for the loss of variance from the use of regression in equation (1), an error term e randomly sampled from a t-distribution with n-2 degrees of freedom is introduced to each of the ranked expected peakflow $\widehat{Y}_j$ to produce a ranked and corrected expected peakflow $\widetilde{Y}_j$ with $\widetilde{Y}_j = \widehat{Y}_j + e$ (Alila et al., 2009). This procedure is iterated 10,000 times in a Monte Carlo simulation to provide a mean of the ranked and corrected-expected peakflow $\overline{\widetilde{Y}_j}$. Following the method described in Alila et al. (2009), confidence limits on the expected peakflow frequency curves are estimated to account for a combination of predictive uncertainty in the calibration equation (1) and the quantile sampling variability, assuming the overall uncertainty is normally distributed. Although confidence limits on the frequency curves were estimated and plotted, our discussion of the analysis outcome does not report the effects of harvesting on the magnitude of Q_p as being important only if they are statistically significant, because what is statistically insignificant could be physically and practically significant (Johnson, 1999). Since nine pairs of watersheds are being investigated concurrently (i.e. meta-analysis), the analysis focuses on whether the upper tails of the frequency distributions of peakflows are displaying similar patterns regardless of post-harvest sample size. This will assist in identifying physically meaningful treatment effects even if they are not necessarily statistically significant, as suggested by Lewis et al. (2010) and adopted by Green and Alila (2012).

The observed peakflows are adjusted to remove the effect of hydrologic recovery to meet the stationarity assumption of the peakflow frequency analysis. Using the chronologically paired Q_p, the "time since end of treatment" $t_{harvest}$ is introduced into the linear regression as a covariate to represent the recovery effect:

$$\widehat{Y}_i = b_0 + b_1 X_i + b_2 * t_{harvest}, \tag{5}$$

This de-trending procedure, which involves subtracting the time component from the observed peakflows, has been used in Alila et al. (2009), Green and Alila (2012), and Thomas and Megahan (1998) to produce a stationary peakflow time series in the post-treatment period for the frequency analyses.

3. Results

In this section, the treatment effects (from harvesting and/or roads) are first reported in the form of changes to sample statistics (mean and variance) of peakflow (Q_p) (Table 2). The coefficient of variation (CV) of the peak-over-threshold (POT) series of the control watersheds is presented in Section 4.1.2 rather than here, because it serves as interpretive evidence for the synchronization and fog-interception mechanisms rather than as a measure of treatment effect.

The analysis of peakflow response in the form of changes to event frequency is important to the understanding of the physical processes. Treatment effects on the Q_p magnitude and frequency are inferred from changes in the form of the frequency distribution (i.e., Cumulative Distribution (CDF) and Probability Distribution (PDF) Functions). In terms of observed peakflows in the form of either CDF or PDF, which again reflect harvesting effects, we present curves both with and without adjustment for recovery effects due to forest regrowth. The implications of the hydrological recovery effects will be discussed separately in subsection 4.2. Overall, watersheds in Coyote Creek and Fox Creek illustrate higher treatment effects than watersheds in Fox Creek and H.J Andrews with similar treatments (harvest cut rate and road density).

3.1. Coyote Creek and Fox Creek

At the Coyote Creek watersheds, the effect of treatment on the mean of Q_p increased with harvest rate: 30% patch-cut in Coyote Creek watershed 2 (CC2) caused a 35.4% increase in the mean, 50% selection cut in CC1 caused a 50.3% increase in the mean, and 100% clearcut in CC3 caused a 85.5% increase in the mean. The effect of forest harvesting on the variance of Q_p in Coyote Creek also increased with cut rate: 52%, 135.9%, and 154% increase in variability in CC2, CC1, and CC3, respectively. Although treatments at Coyote watersheds were designed with different road densities, the experimental design within the site does not allow the isolation of the effect of roads from the effect of tree removal. At Fox Creek sites, however, the two watersheds (FOX1 and FOX3) have similar harvest rates (25% patch-cut) but different road densities (2.1 km/km^2 in FOX1 and 1.3 km/km^2 in FOX3). The increase in the mean of Q_p was 20.9% in FOX1 and 4.7% in FOX3. The increase in Q_p variability was 82.9% in FOX1 and 34% in FOX3.

CDFs and PDFs of Coyote Creek and Fox Creek watersheds are plotted in Figure 4 and Figure 5, respectively, for the assessment of changing event magnitude and frequency. At Coyote and Fox Creek sites, forest harvesting increased the magnitude of all Q_p regardless of size (illustrated by the entire observed Q_p CDFs shifting upward compared with the expected Q_p CDFs). Remarkably, the effect of harvesting on the magnitude of Q_p increased with event size (illustrated by vertical differences between the observed and the expected CDFs increasing with return period). Harvesting in Coyote and Fox Creek watersheds also increased the frequency of all peakflow events, irrespective of magnitude. (See insets of Figure 4 and Figure 5.) In Coyote Creek, for instance, 100% clearcut with roads has caused a four to five times increase in Q_p frequency in CC3 (e.g., a 30-year event becoming ~7-year event), 50% selection cut with roads caused a three to four times increase in Q_p frequency in CC1 (e.g., a 30-year event becoming ~8-year event), and 30% patch cut with roads almost doubling the Q_p frequency in CC2 (e.g., a 10-year event becoming a 6-year event). At Fox Creek, interestingly the relatively lower cut rate (25% patch-cut) has resulted in two to eleven times increases in the peakflow frequency, with the larger events showing an even larger increase in frequency (e.g., 10-year events turning into 1- to 3-year events and 30-year events turning into 3- to 4-year events).

The split-season analysis (ROS dominant months versus non-ROS dominant months) in Fox Creek and Coyote Creek indicated that, in these watersheds, the treatment signal was most pronounced in the variability and in the upper-tail behaviour of the ROS-dominant months relative to the combined non-ROS months (Figure 6). For CC3 (100% cut

Table 2
Relative change in sample statistics with full record length and similar record length comparison. HJA watersheds have their record length reduced to match Coyote and Fox Watersheds on the right-hand side of the table to provide an inter-group comparison without the effects of sample size and length of observation.

Sites	Pair (Treatment-Control)	Full available Record Length					Similar Cross-site Record Length				
		Relative Change of Q_p Mean (%)		Relative Change of Q_p Variance (%)		Post-Treatment Record Size (Year)	Relative Change of Q_p Mean (%)		Relative Change of Q_p Variance (%)		Post-Treatment Record Size (Year)
		With Recovery	Recovery Adjusted	With Recovery	Recovery Adjusted		With Recovery	Recovery Adjusted	With Recovery	Recovery Adjusted	
Coyote	CC1-CC4	35	50.3	116.2	135.9	22	35	50.3	116.2	135.9	22
Coyote	CC2-CC4	23	35.4	35.7	52	22	23	35.4	35.7	52	22
Coyote	CC3-CC4	55	85.5	121.2	154	22	55	85.5	121.2	154	22
Fox	FOX1-FOX2	19	20.9	59.9	82.9	17	19	20.9	59.9	82.9	17
Fox	FOX3-FOX2	4.6	4.7	33.8	34	17	5	4.7	33.8	34	17
HJA	HJA1-HJA2	30	38.7	-10.1	3.3	47	28	28.4	-19.4	-18.7	23
HJA	HJA3-HJA2	12	12.2	-8.4	-8.5	50	18	22.3	-11.6	-4.4	25
HJA	HJA6-HJA8	21	35.2	7.2	25.4	39	17	16.5	17.1	17.1	22
HJA	HJA10-HJA9	8.9	8.9	7.2	9.3	38	5	4.6	-0.5	-7.1	21

rate with roads), the increase in the mean is 107% during ROS-dominant months and 58% during non-ROS-dominant months; and the change in the variability is 223% and 22%, respectively. In the case of FOX3 (25% cut rate with roads), changes in the mean Q_p between ROS and non-ROS dominant months are similar, 3% and 3.5%, respectively. However, the response in terms of the variability is drastically different between the two: 28.5% during ROS dominant months and -6.6% during non-ROS dominant months. In CDF comparisons of both CC3 and FOX3, the vertical difference between observed and expected CDF of the non-ROS dominant months is relatively smaller compared with ROS dominant months. The vertical difference also remains relatively constant with increasing return period for the non-ROS dominant months but shows a strong increasing trend in ROS dominant months. One caveat is that the non-ROS sample combines early-wet-season months (September–October) with late-wet-season months (March–May), which differ in antecedent soil-moisture conditions: after the dry summer, the difference in soil-moisture deficit between treated and control watersheds is largest in early fall and probably smaller in spring. Because these sub-seasons are aggregated, the non-ROS treatment difference reported here is an average across hydrologically distinct periods; disaggregating them is a worthwhile direction for future analysis.

3.2. H.J. Andrews

At the H.J. Andrews site, there are four treatment watersheds, with HJA1, HJA3, HJA10 being adjacent to each other and sitting at the southwest corner of the Experimental Forest; and with HJA6 sitting across the Experimental Forest at the northeast corner, higher in elevation. Although HJA10 is adjacent to HJA1 and HJA3, HJA10 is different because it is about 10 times smaller and has a lower elevation range. For HJA1 (100% clearcut, no roads) and HJA3 (25% patch-cut, with roads), differences in treatments resulted in different increases in the mean (39% in HJA1 and 12% in HJA3) and different changes in the variability (3.3% in HJA1 and -8.5% in HJA3). Frequency analyses (CDFs and PDFs in Figure 7) illustrate the increase in the peakflow magnitude of smaller peakflows (with return period < 10-year) in these two H.J. Andrews watersheds. For peakflows larger than 10-year, notably overlapping observed and expected CDFs of HJA1 and HJA3 suggest that larger events are not affected by treatments in these two H. J. Andrews watersheds. In terms of change in the peakflow frequency, smaller peakflows in HJA1 are doubled in frequency (10-year becoming ∼4-year event) and no change in frequency for events larger than 10-year. Similarly, in HJA3, the frequency of smaller peakflows is increased by 30% with no change in the frequency of the larger peakflows.

In terms of treatment level, HJA1, HJA6, and HJA10 have the same cut rate (all 100% clearcut) but with HJA6 having additional treatment effects from forest roads. The increases in the Q_p mean were 35% for HJA6 and 9% for HJA10; and the increases in the variability were 25.4% for HJA6 and 9.3% for HJA10. The vertical difference between CDFs in the frequency analysis shows that magnitudes of Q_p increased for all return periods in HJA6 and HJA10 (Figure 7) and, unlike HJA1 and HJA3, such vertical differences increased with return period without a no-effect threshold, suggesting larger treatment effects on events larger than 10-year. The increasing vertical difference of CDFs with return period can also be translated into a larger increasing Q_p frequency with larger events. In HJA6, the 10-year and 50-year events become 1.6 and 2.6 times more frequent, respectively (10-year and 50-year become ∼6-year and ∼19-year events, respectively). In HJA10, the change in frequency for a 50-year event is 2.5 times (50-year becoming ∼20-year), although such a difference could be caused by the largest two observations being more sensitive to the ranking uncertainty. Since the general climate conditions are the same for the four watersheds of H.J. Andrews, judging by the responses of post-treatment peakflow frequency curves between watersheds, the contrasting treatment sensitivity of the large events (either low sensitivity as in the case of HJA1 and HJA3 or high sensitivity as in the case of HJA6 and HJA10) needs to be understood through the physical processes of how watershed physiographic characteristics influence treatment effects.

4. Discussion

In this section, the inter-site comparisons of the sensitivity of the peakflow regime to treatment among Coyote Creek, Fox Creek, and H.J. Andrews are explored through the use of stochastic understanding.

4.1. Process Controls of Sensitivity of Peakflow to Treatment: Inter-site Comparison

At first glance, the treatment sensitivity appears to be erratic. Among all watersheds observed across the three sites, the four treatment watersheds that received 100% clearcut experienced increases in the mean of Qp ranging from 9% to 86% and in the variability of Qp from 3% to 154%. The four treatment watersheds subject to moderate cut rates (25 and 30% harvesting) experienced increases in the mean of Qp of 5% to 35% and changes in the variability of Qp of −9% to 52%. An immediate observation is that the increase in the mean and variability tends to be larger in Coyote Creek and Fox Creek than in H.J. Andrews when the treatment is similar. For example, the treatment effect in HJA1 (100% clearcut, no roads) is smaller than in CC3 (100% clearcut, with roads), even though roads in CC3 may be a confounding factor. HJA3 has a treatment similar to the two Fox Creek watersheds (25% patch-cut, with roads), yet the effects on the larger events (>10 year) are drastically different: no effect in HJA3 but a 10 to 30% increase in peakflow magnitude in FOX1 and FOX3.

These relative changes in the mean and variability of Qp across all

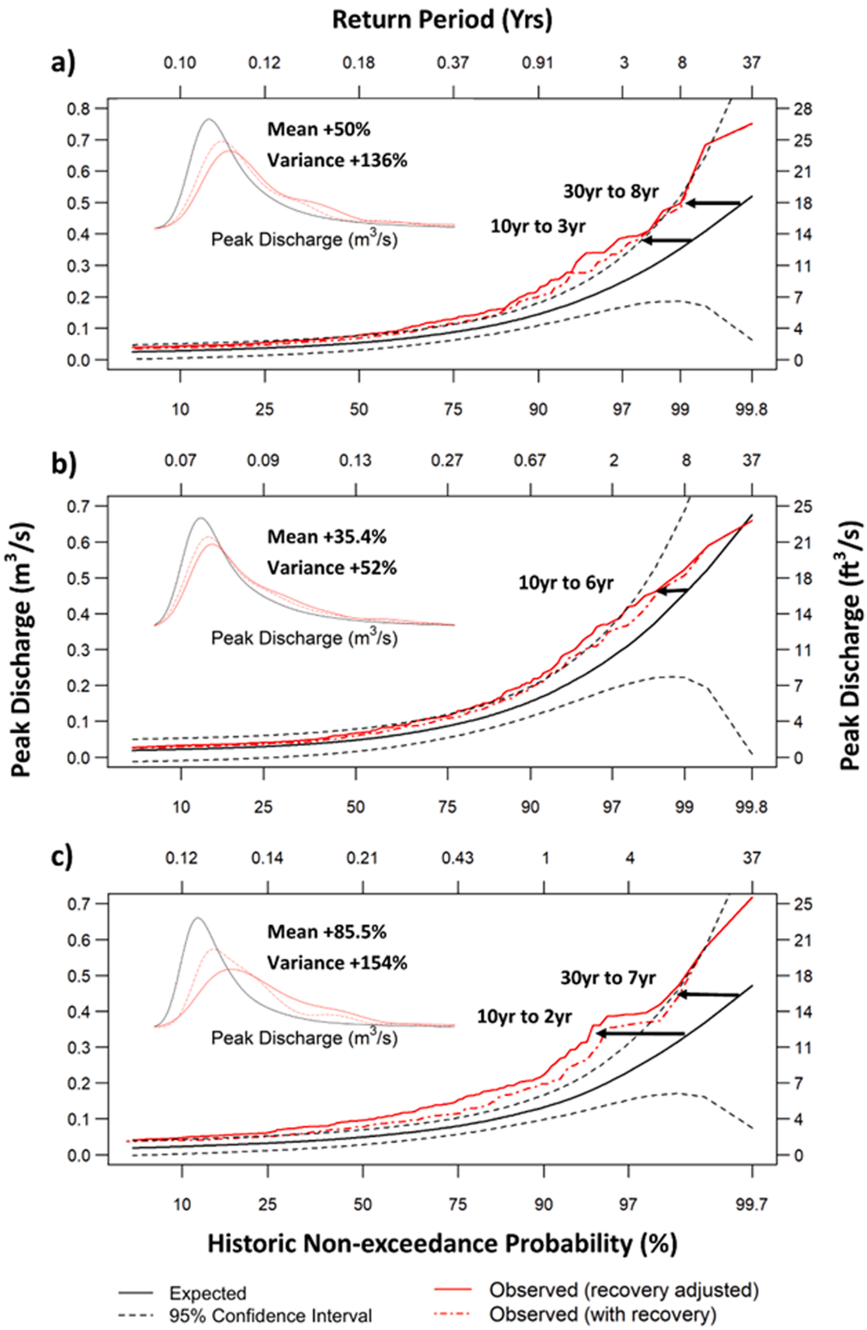

Figure 4. Cumulative Distribution Function (CDF) of post-treatment peakflows: a) Coyote Creek CC1 (with CC4 as control), b) Coyote Creek CC2 (with CC4 as control), and c) Coyote Creek CC3 (with CC4 as control). Inset graphs are the Probability Distribution Function (PDF) of post-treatment peakflows for the two respective watersheds. The thin black solid lines in CDF and PDF graphs represent the expected peakflows, calculated using the calibration function developed with pre-treatment peakflows. The red lines represent raw observed peakflows in the treatment watersheds and are affected by hydrological nonlinearity caused by the vegetation regrowth after harvesting. The dashed lines represent observed peakflows with the hydrological recovery effects adjusted. The inset data show changes in magnitude (% change) and return period of some larger peakflows. The change in frequency is interpreted as, for example, the treatment changing the 30-year event of CC1 into an 8-year event (almost 4 times more frequent).

nine pairs are summarised in Figure 8, which anchors the comparison developed below. To make the reasoning traceable, the following subsections take the six hypotheses of Section 1.3 in turn: elevation-controlled snowmelt synchronization (H1, Section 4.1.1); the suppression of fog interception in humid environments (H3, Section 4.1.2); the additional local controls exerted by a drier climate and by the road network (H4 and H2, Section 4.1.3); and the resulting behaviour of the large, infrequent peakflows at the upper tail (H5 and H6, Section 4.1.4). Section 4.2 then synthesises these controls. Each subsection closes by stating whether its hypotheses are supported by the evidence.

4.1.1. *Elevation Range and Snowmelt Synchronization (Hypothesis 1)*

Hypothesis 1 holds that a watershed's elevation range governs the spatial synchronization of runoff generation through the snow mass and energy balance, so that greater synchronization produces a larger post-harvest increase in the mean and variability of peakflows.

In terms of physiographic characteristics, what makes HJA1 and HJA3 distinctive compared with the other treatment watersheds is their larger elevation range. We hypothesized that the mechanistic WAR desynchronization over space and time reduces the mean and variability of peakflows. Such desynchronization at the watershed scale is increased

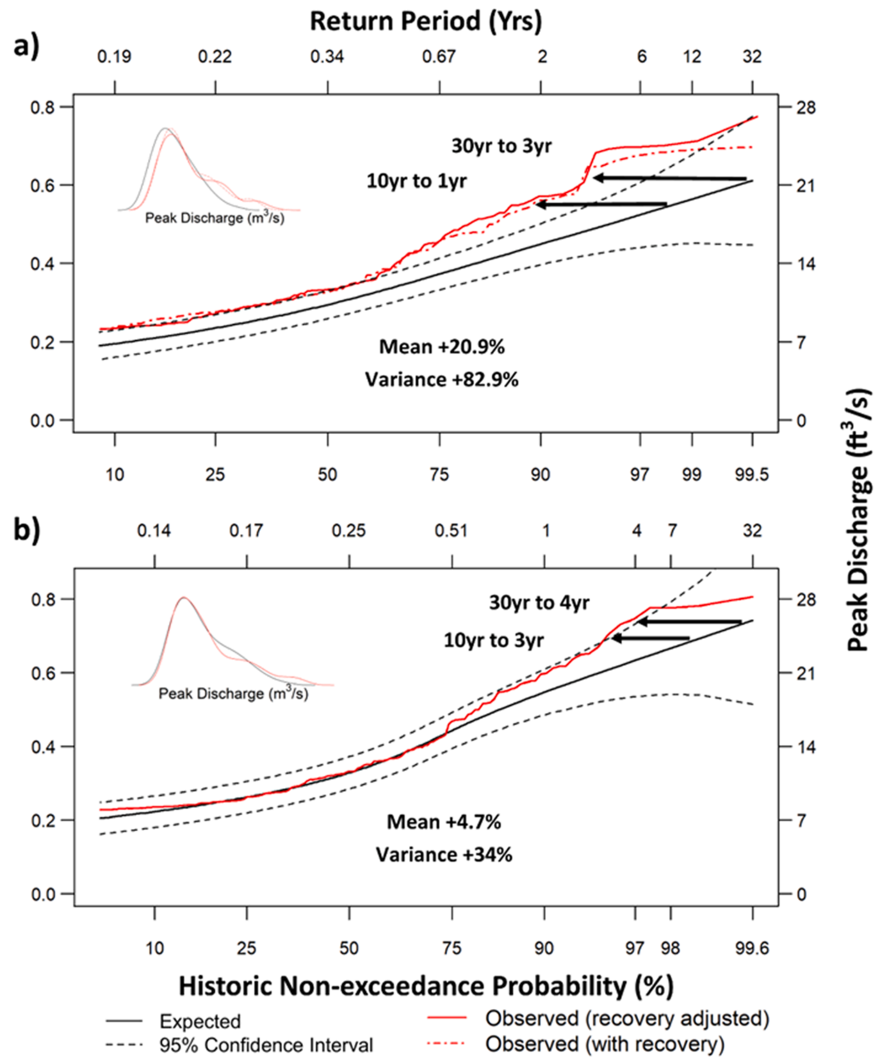

Figure 5. Similar to Figure 4. Cumulative Distribution Function (CDF) of post-treatment peakflows: a) Fox Creek FOX1 (with FOX2 as control) and b) Fox Creek FOX3 (with FOX2 as control). There is a distinct change of variability between peakflows smaller and larger than the return period of around 0.5 year (shown as changes in the CDF slope) for both FOX1 and FOX3. Increase of peakflow frequency (reduction of return period) increases with peakflow size.

by spatial heterogeneity of SWE mass and energy balance where the watershed has a larger elevation difference between its ridges and its mouth. Based on the stand-level snow mass and energy balance understanding of Garvelmann et al. (2015), the removal of forest canopy exposes the snow to greater variability in the climatic controls; consequently, a clearcut watershed with a large elevation range (such as HJA1) can experience more WAR desynchronization. In the case of HJA3, the locations of the patch-cut blocks introduce further sources of desynchronization: there are three discrete cut blocks, each about 8% of the total watershed area, two at mid-elevation and the third near the outlet, so that runoff generation is desynchronized between (i) the cut blocks and their adjacent forest, (ii) the three cut blocks situated at different elevations, and (iii) the forested areas at different elevations. Greater desynchronization of WAR in HJA1 and HJA3 after harvesting should therefore lower the probability of occurrence of larger peakflows at the outlet, counteracting the stand-level increase in WAR caused by higher SWE and ablation rates following harvesting.

Our pre- and post-harvesting peakflow frequency analyses at HJA1 and HJA3 suggest that this desynchronization-driven lowering of the mean and variability may not completely, but can substantially, counteract the stand-level increase. This is consistent with our findings, though Bathurst et al. (2020) analyzed a 7-year post-harvest record at HJA3, and observed diverging pre- and post-harvest flood frequency curves, suggesting initial runoff synchronization, likely reflecting the short record's inability to capture the full manifestation of desynchronization effects. Although hydrologists have long understood arrival-time desynchronization through deterministic single-event hydrographs, such watershed-scale desynchronization effects on peakflow frequency are discernible only within a probabilistic framework.

In contrast to the high elevation ranges of the steep HJA1 and HJA3 watersheds, the topography of Coyote Creek and Fox Creek is relatively subdued. In snowmelt-dominated regions of British Columbia, peakflows in subdued watersheds exhibit higher variability than in steep mountainous watersheds, a phenomenon attributed to synchronized melting (Green & Alila, 2012); similar processes are plausible in the ROS environment, since spatial homogeneity of the pre-event snowpack also promotes synchronized melting and hence synchronized WAR generation across the watershed. The coefficient of variation (CV), a dimensionless measure of peakflow variability about the mean, is most informative as a like-for-like comparison among control watersheds; for quantifying treatment effects, the harvest-induced shift in peakflow frequency is a more direct and reliable indicator than a change in CV. Comparison of the CV of the POT series of the control watersheds (CC4, FOX2, HJA2, HJA8, and HJA9) reveals that Coyote Creek and Fox Creek behave unexpectedly differently. The CV of CC4 (the control for CC1, CC2, and CC3) is 1.08, higher than those of the steep H.J. Andrews

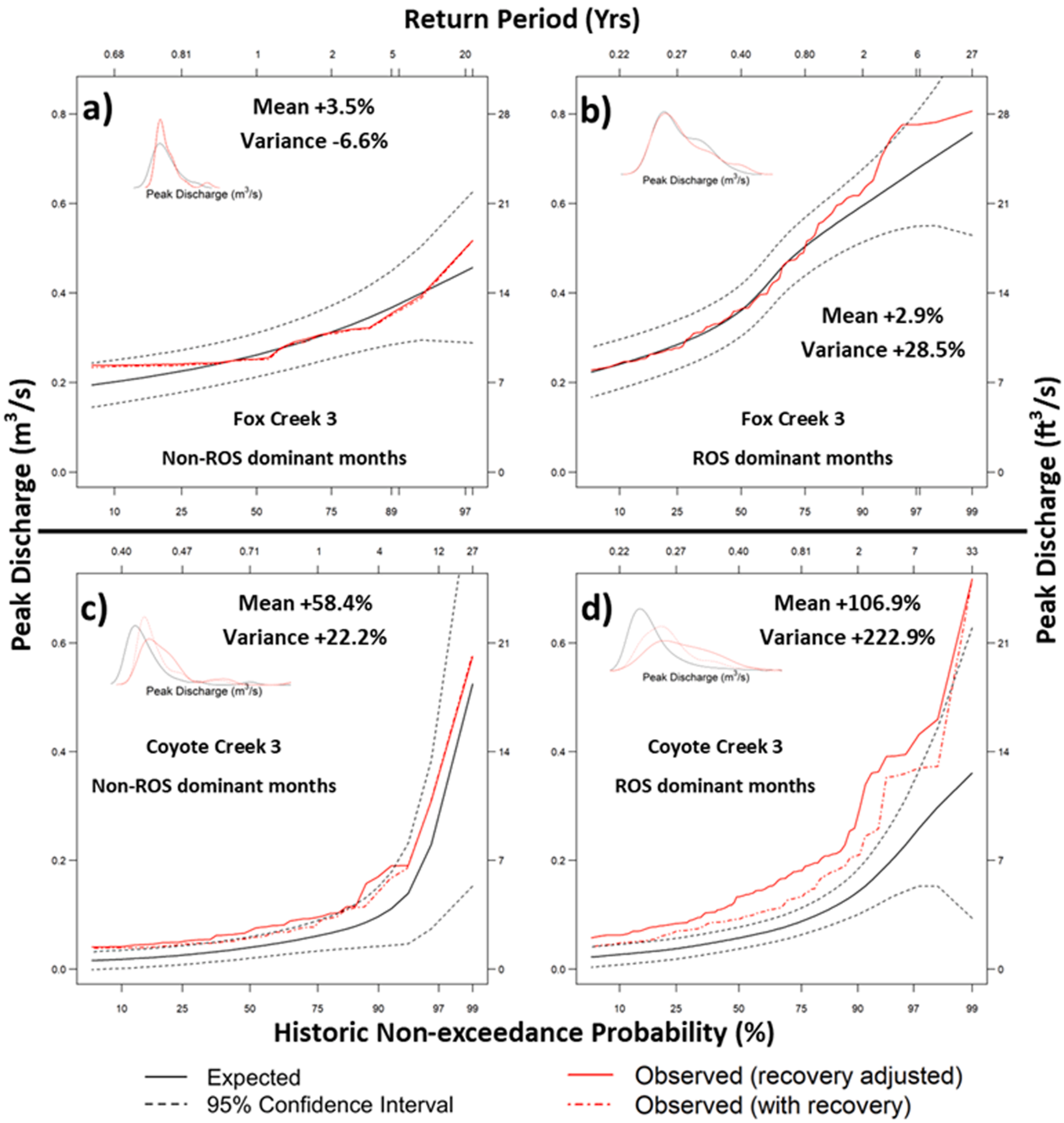

Figure 6. Cumulative Distribution Function (CDF) of post-treatment peakflows with split samples. The samples are split into non-Rain-on-Snow (non-ROS) dominant months of the wet season (September, October, March, April and May, shown on the left) and Rain-on-Snow (ROS) dominant months (December and January, shown on the right). November and February are treated as transition months and are excluded from both groups; although snow can fall in these months, fresh snow during these energy-rich transition periods typically melts rapidly, so the event type is ambiguous. Top panel: Fox Creek FOX3. Bottom panel: Coyote Creek CC3. The insets show the PDFs and changing sample statistics of the recovery-adjusted peakflows.

controls (0.42 to 0.81); this is expected, both because of synchronized runoff generation in a subdued watershed (Green & Alila, 2012) and because of the drier hydro-climatology of Coyote Creek relative to the other two sites (Figure 3), as meteorological conditions are themselves more variable in drier environments (Merz & Blöschl, 2009).

Taken together, H1 is supported: the large elevation ranges of HJA1 and HJA3 coincide with the muted post-harvest shifts expected from WAR desynchronization, while the subdued Coyote Creek control shows the elevated pre-harvest variability expected where desynchronization is weak. The one apparent exception concerns Fox Creek, whose control records the lowest CV (0.38) of any watershed in this analysis, contrary to the expectation that its subdued, elongated form would synchronize runoff and raise variability. This anomaly motivates the fog-interception mechanism examined next.

4.1.2. *Fog Interception in Humid Environments (Hypothesis 3)*

Hypothesis 3 holds that, in certain humid environments, tree removal suppresses fog interception, increasing the mean and variability of peakflows through a higher baseflow and an intensified ROS response, and thereby rendering such environments among the most sensitive to harvesting.

Why is the peakflow variability so low in the Fox Creek control, and, more importantly, how is such a low control CV associated with the comparatively large post-harvest increase in variability at FOX1 and FOX3? The more elongated shape of the Fox Creek watersheds (Jones, 2000; Figure 4) could desynchronize peakflow generation through the drainage-network geometry. Yet, as a holistic observation, the much lower CV of FOX2 (control) relative to the other controls is not fully explained by this effect, and such geometry-induced synchronization should not itself be much altered by harvesting and so cannot explain the large post-harvest increase in variability. It is therefore hypothesized that an additional mechanism reduces peakflow variability in this region. The 30% greater annual water input to forested than to clearcut stands in Fox Creek (Harr, 1982; Ingwersen, 1985) could produce both

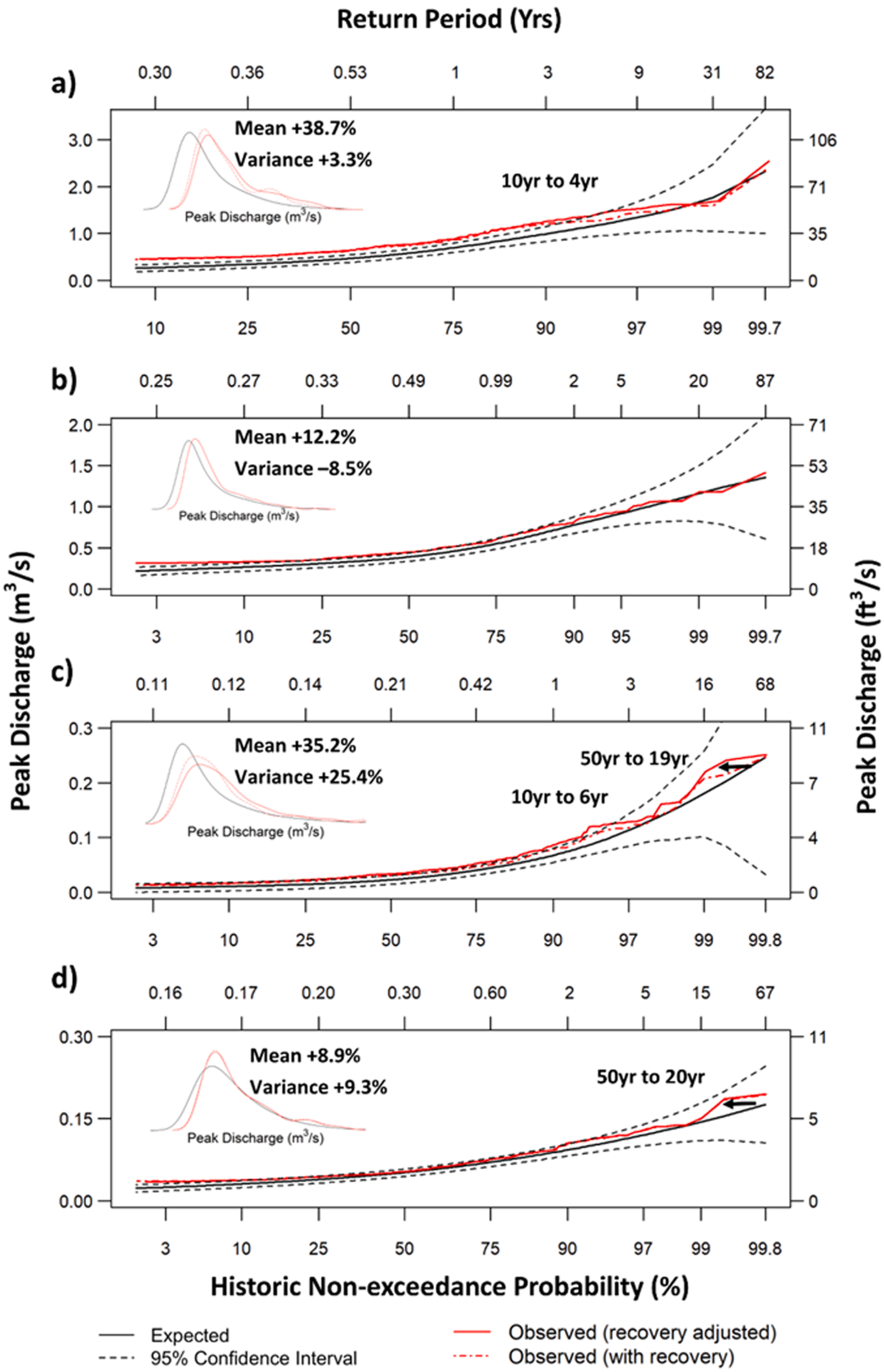

Figure 7. Similar to Figure 4. Cumulative Distribution Function (CDF) of post-treatment peakflows: a) H.J. Andrews HJA1 (with HJA2 as control), b) H.J. Andrews HJA3 (with HJA2 as control), c) H.J. Andrews HJA6 (with HJA8 as control) and d) H.J. Andrews HJA10 (with HJA9 as control). The post-treatment CDF converges with expected CDF, resulting in a non-significant increase of peakflow magnitude for large peakflows (return period > 10 year) in HJA1 and HJA3.

observations, the low control variability and the large post-harvest increase. Fog drip has been documented along the mountainous ridges of Oregon and California, producing notable differences in annual precipitation (Ingraham & Matthews, 1995; Isaac, 1946) with events lasting for days and seasonal collection totalling as much as 42.5 cm (Azevedo & Morgan, 1974). First, fog interception increases water input to the forested control (a mass-balance effect), raising baseflow and thereby reducing CV (Blöschl & Sivapalan, 1997); this recharge is most pronounced in early fall when soils are dry (Jones, 2000). Second, fog-derived water during winter can further reduce CV through an energy-balance effect, adding energy to the snowpack beneath the canopy and limiting its development so that it contributes less to ROS runoff, analogous to meltwater drip, which is known to add energy to the sub-canopy snowpack in ROS environments (Berris & Harr, 1987;

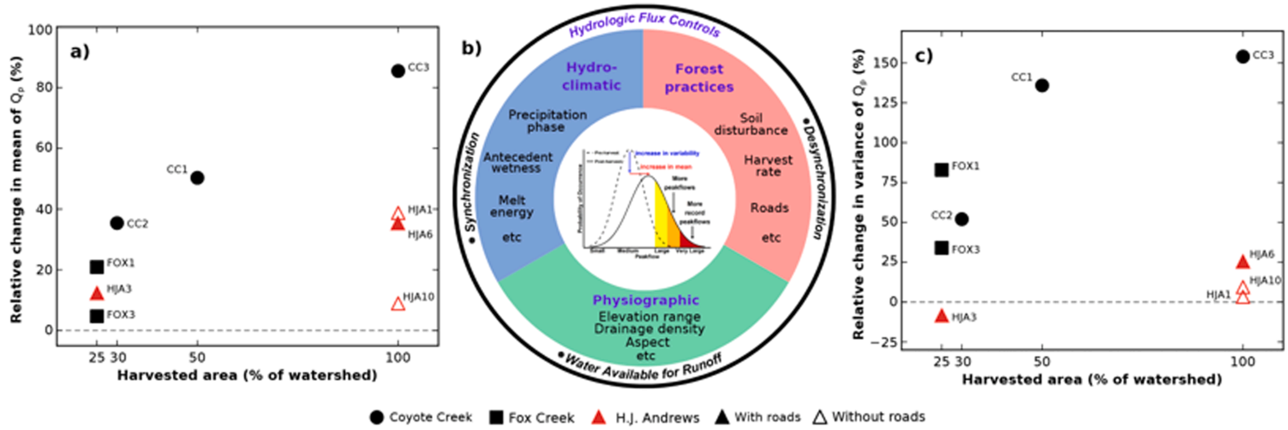

Figure 8. Relative change in the (a) mean and (c) variance of post-harvest Qp, in comparison to the relative harvest area of the watershed, for all nine watersheds. Panel (b) shows the controls on the peakflow magnitude-frequency relation, while the outer ring shows the hydrologic mechanisms through which they act. Although larger cut rates tend to produce larger increases in the mean and variance, the relationship is multivariate, rather than driven by harvest rate alone; the H.J. Andrews watersheds (shown in red) illustrate this, with their individual responses discussed in Section 4.1.5. Skewness may also change with harvesting, but is not shown, owing to the large uncertainties in estimating third-order moments.

Storck et al., 2002). While direct quantification of fog and meltwater drip as energy sources remains limited, the physical reasoning is consistent with the peakflow frequency curves of FOX1 and FOX3, lending empirical support to the significance of fog-drip energy. The treatment effects (the vertical difference between CDFs) on small Qp events (return period < 0.5 years) are distinctly smaller than those on larger events (return period > 0.5 years) at Fox Creek (Figure 5); in the case of FOX3, there is no treatment effect for small events at all. Because the energy-balance contribution of fog drip is negligible during the more rain-dominated seasons, the reduction in fog interception following harvesting reduces rain-only runoff mainly through its mass-balance effect (less water input). This is further supported by the split analysis of FOX3, which shows no significant treatment effect during non-ROS-dominated months (Figure 6). The energy-balance effect of the extra dripped water becomes increasingly important as snowmelt contributes more to runoff in mid-winter: reduced pre-event energy input following harvesting leads to higher snow accumulation and subsequently higher WAR, an effect that appears significant only at the peak of the ROS season, where the FOX3 split analysis shows large treatment effects confined to the few largest events.

H3 is therefore supported: the documented fog-drip surplus to forested Fox Creek stands is consistent both with the anomalously low control watershed CV and with the large post-harvest increase in variability at FOX1 and FOX3, identifying the suppression of fog interception as the mechanism that makes these humid watersheds among the most sensitive to harvesting.

4.1.3. *Local Controls on the Magnitude of the Response: Climate and Road Networks (Hypotheses 4 and 2)*

Beyond elevation-driven synchronization, two local controls modulate the magnitude of the response. Hypothesis 4 holds that, within the snow-transient zone, drier-climate watersheds are more harvest-sensitive; Hypothesis 2 holds that a denser road network raises routing efficiency and synchronization, increasing the mean and variability of peakflows.

At Coyote Creek, the larger post-harvest variability increase appears driven by the drier, more variable climate, with the ROS/non-ROS split (Figure 6) locating the sensitivity in altered mid-winter snowpack dynamics. Fog suppression makes the humid Fox Creek watersheds sensitive mainly through a reduced return period (a frequency effect), whereas the drier Coyote Creek climate acts mainly through increased magnitude, widening the vertical gap between the frequency curves of Figure 4. These two routes (magnitude versus frequency) are distinct, a counter-intuitive result that only the stochastic framework exposes, and consistent with the dictum that watersheds with milder-sloped pre-harvest frequency curves are the most sensitive (Berris & Harr, 1987; Alila et al., 2009; Johnson & Alila, 2023; Kaluarachchi & Alila, 2025; Pearson-Atkins et al., 2026; Pham et al., 2025).

H4 is supported within the snow-transient zone: among comparable treatments, the drier, more variable Coyote Creek climate produces the largest increases in the mean and variability of Qp (Merz & Blöschl, 2009).

Roads are the second control. Since FOX1 and FOX3 are physically alike and equally harvested, the larger increase at FOX1 follows from its higher road density. In a probabilistic framing, this parallels the drainage-density effect of ditching, though drainage ditches raise drainage density by an order of magnitude more than roads alone (Robinson, 1986, and references therein), while roads reduce response time and enhance synchronization.

H2 is supported as predicted: with physiography, climate, and cut rate held constant, FOX1's higher road density yields the larger increase in the mean and variability of Qp relative to FOX3.

4.1.4. *Magnitude and Frequency of Large Peakflows (Hypotheses 5 and 6)*

The preceding controls act on the mean and variability of the whole distribution; their effect on large, infrequent events is the subject of Hypotheses 5 and 6. H5 holds that infrequent peakflows (return period > 10 years) can be substantially affected as a direct consequence of those changes; H6 holds that, within the observed records, the effect can increase unchecked with event size, with no apparent 'no-effect' threshold.

Because a change in the mean and variability rescales the whole distribution, its imprint reaches the infrequent events. At the synchronization-dominated sites (Coyote Creek, Fox Creek, HJA6) the pre- and post-harvest curves keep diverging into the upper tail (Figure 8b), so the absolute increase for infrequent ($>$10-year) events is at least as large as for frequent ones; the upper-tail confidence is treated in section 4.3. The desynchronized steep watersheds show no such amplification: HJA3 shows no effect on its $>$10-year events while comparably treated Fox Creek watersheds increase by 10–30%. H5 is therefore supported at the synchronization-dominated sites but not where desynchronization dominates, a distinction visible only in the probabilistic framework.

Within the 17 to 50-year post-harvest records, the curves at the synchronization-dominated sites show no convergence toward a common bound: no return period marks an end to the effect, and the separation tends to grow with event size. H6 is therefore supported under synchronizing conditions (subdued topography, roads, drier climate) but not universally; where desynchronization dominates (HJA1, HJA3) the effect is bounded, even diminishing at the largest events. That identical harvesting can produce an unchecked increase in one watershed and a near-zero effect in another is not a contradiction but a central result: the upper tail is governed by how macroscale physiography and climate organize WAR delivery, not by cut rate alone.

4.2. Forests Owe Their Causal Power on Peakflows to Physiography and Climate

Treatment sensitivity is multivariate, not a function of cut rate alone (Figure 8). Harvesting reshapes the peakflow regime through the mean and variability of Qp, and these two changes determine the effect on magnitude and frequency, especially at the upper tail (Figure 8b). Despite identical 100% clearcuts, HJA1 responds weakly (mean +38.7%, variance +3.3%) because it has no roads, a large elevation range, and a humid climate, while CC3 responds strongly through its subdued topography, roads, and drier climate. HJA3 (25% cut) is similarly muted (mean +12.2%, variance -8.5%) for the same physiographic reasons, whereas the Fox Creek watersheds at the same cut rate are highly sensitive because fog suppression lowers their pre-harvest variability. Within H.J. Andrews, HJA6 (subdued, mean elevation near peak-ROS) responds most (mean +35.2%, variance +25.4%) and HJA10 least (mean +8.9%, variance +9.3%; steep, low, no roads). Roads, present throughout Coyote and Fox Creek but not all of H.J. Andrews, further widen the gap.

Stand-level deterministic mechanisms (evapotranspiration, canopy interception, snow shading) have long explained forest effects on peakflows, but our results show them insufficient: macroscale physiography and climate are decisive. What distinguishes the responses is how forest practices interact with these controls to synchronize or desynchronize WAR delivery (Figure 8b). Because each watershed combines the controls differently, identical stand-level mechanisms integrate differently in space and time, making sensitivity watershed-specific (Beven, 2000). This is why the comparison looked erratic at the outset and resolves only when the nine pairs are read together through a stochastic, causal framework: one pair can suggest macroscale control (Johnson & Alila, 2023; Pearson-Atkins et al., 2026) and two can begin to test it (Pham et al., 2025), but nine provide far stronger grounds. That a system's causal power lies at its macroscale rather than microscale is not unique to hydrology; it recurs across the sciences, from systems biology to philosophy, across more than a dozen measures of causation (Comolatti & Hoel, 2022; Flack, 2017; Hoel et al., 2013; Rosas et al., 2020). Forest hydrology belongs within this understanding: the causal power of forests on peakflows is governed at the watershed scale, by physiography, climate, and cut-block distribution, not at the stand scale.

4.3. Hydrological Recovery

Trees regrow after harvesting, so quantifying the effects immediately after harvesting has practical limitations. However, it is a critical first step, since the pace of recovery cannot be estimated without first correctly quantifying the initial effects from which recovery proceeds. Although the primary focus of this study is to quantify the hydrologic effects immediately after harvesting, we do recognize there is a practical need to assess the pace of hydrological recovery because it determines the length of heightened risk exposure and has tremendous influence on how professionals assess overall risk and reliability over a longer term. The experimental design of this study (namely the stationary frequency analysis coupled with a de-trending technique) was not designed to investigate recovery specifically. We will, however, offer some observations from our de-trending exercise to illustrate the contradiction in the conclusions of the pace of hydrological recovery between a probabilistic framework and the full deterministic ANOVA/ANCOVA framework (Beschta et al., 2000; Thomas, 1990; Thomas & Megahan, 1998).

The exercise reported in Table 2 purposefully reduces the record length of some longer records in H.J Andrews to match the record sample size of other studied watersheds. The differences in the amount of recovery adjustment (which is the vertical difference between adjusted and unadjusted series) between the shorter sample set and longer sample set could be considered as an indirect representation of the hydrological recovery in the four H.J. Andrews sites. First, adjustment for recovery in HJA1 with a shorter record length of 23 years shows no significant difference in either change of the mean or variability of Q_p relative to the expected. Then, with the full record of 50 years of observations, the change in the mean and variability of Q_p relative to the expected are significantly different between the recovery-adjusted and unadjusted records. Because the adjustment for recovery is only significant for a record length of 50 years but not for 23 years, it is reasoned that significant and detectable hydrological recovery does not occur until some 20 years after the initial treatment effects. This conclusion contradicts the conclusion drawn from a deterministic analysis by Thomas and Megahan (1998), who claimed significant hydrological recovery in the first, third, and fourth decades in the post-treatment period with the first decade showing the fastest recovery, and for no apparent physical reasons there is no recovery in the second decade. Consider the vegetation recovery rate in this region, which is about 60% in 30 years for canopy cover and LAI (Jones & Grant, 1996). We postulate that there is little if not zero hydrological recovery in the first two decades following clearcutting of the watershed. This aligns with the findings of Crampe et al. (2021), who indicate no clear evidence of hydrologic recovery 50 years post-harvest at H.J. Andrews. A similar conclusion of no significant recovery for the first two decades after treatments is also found in HJA6 for both i) changes in the mean and ii) changes in the variability of Q_p. Namely, there is no significant recovery found by the recovery adjustment exercise using the arbitrarily shortened record (22 years post-treatment). There is, however, at least some recovery significant enough to be detected when using the full record (39 years post-treatment). The same exercise for HJA3 is inconclusive, possibly due to several confounding factors such as time-sensitive desynchronization caused by scattered cut-blocks and time-independent synchronization caused by roads. The record of 17 years at Fox Creek also requires almost no recovery adjustment, which is consistent with the hypothesis that little recovery happens in the first two decades following treatment. Therefore, from our observations in the H.J. Andrews watersheds, we find no support for the notion of fast hydrological recovery proposed in the traditional deterministic analyses of Thomas and Megahan (1998).

In Coyote Creek, due to a gap in the discharge time series, although the sample size for post-treatment frequency analysis is only 22 years, the effective recovery period for the three Coyote Creek treatment watersheds is in fact 41 years (1972 to 2013) and the recovery is noticeable. Nevertheless, the amount of hydrological recovery over a period of four decades does not appear to be on the same magnitude as the treatment effects. Stationarity assumption aside, if the unadjusted observed peakflow frequency curve, which confounds treatment effects with hydrological recovery effects, is to be compared with the expected peakflow frequency curve, the increase in Q_p magnitudes is still large (Figures 4 and 6). This suggests that the hydrological response to harvesting and roads could be slow to recover in this region, which echoes previous studies by R.D. Harr and colleagues, whose stand-level outflow experiment observed significant increase of water outflow at the 40-year-old plantation stand compared with the fully forested stand (Harr et al., 1989; Harr & Coffin, 1992). That led them to conclude that hydrological recovery by vegetation regrowth in Rain-on-Snow environments is slow: "so-called hydrologic recovery is only about 50 percent complete in forest plantations approximately 25 years old (Harr et al., 1989, p. 6)". Such findings from a stand-level experiment were mostly dismissed by the forest hydrology community, perhaps because they are inconveniently incompatible with the research outcomes of the few available watershed-level deterministic recovery studies (Beschta et al., 2000).

On the physical processes related to hydrological recovery, the concept of resilient ecosystem is often being used to support why hydrological recovery should be fast in the Pacific Northwest. Often, studies on the topic of hydrological recovery are reductionist in approach: They investigate one at a time the various aspects of such ecosystem resilience, e.g., recovery of vegetation, soil conditions, or how snow dynamics change following regrowth of the forest (Winkler & Boon, 2015). However, since vegetation regrowth and snow dynamics are hard to assess on a larger scale, the discussion of hydrological recovery often relies on an understanding of stand-level processes. Similar to treatment effects, discussion of spatial aggregation and cumulative effects between processes is often missing when in fact the hydrological recovery is occurring on a watershed scale. In this study, we demonstrate how runoff generation can be synchronized or desynchronized by physical characteristics of the watershed, such as elevation range and aspect distribution and/or the treatment itself. How differential vegetation regrowth rates at lower and upper elevations might influence hydrological recovery through the alteration of such synchronization/desynchronization processes is still an open question. For the above spatial, temporal, and process complex interactions, it is the opinion of the authors of this study that the experimental design of watershed-scaled hydrological recovery needs to be understood under a frequency-based nonstationary framework, especially when the effects of harvesting on the magnitude and frequency might be recovering at different rates (Pearson-Atkins et al., 2026). Stochastic methods developed in other disciplines, such as climate science and analytical finance, could potentially free hydrologists from the linear up-scaling of processes (Salas & Obeysekera, 2014). Readers are referred to two recent studies that used frequency pairing under non-stationary conditions for understanding and quantifying the effects of harvesting practices at any point in time during the disturbance history of a watershed in the snow environment and, hence, a direct evaluation of hydrologic recovery of the peakflow regime (Johnson & Alila, 2023; Pearson-Atkins et al., 2026).

4.4. *Meta-Analysis Approach: Confidence in Upper-Tail Predictions*

Estimates of frequencies in the upper tail of sample distribution can be sensitive to sample size which varied in this study from 17 to 50 years. For any record length, there always will be sampling uncertainty associated with the empirically estimated return periods of the largest field-measured or model-simulated peakflows. In this study, the reported changes to frequency caused by forest harvesting were restricted to events smaller than 50-year return periods. The pre- and post-harvest sample peakflow frequency curves are reasonably well-defined for such a range of return periods, for four reasons: i) the emerged consistencies in the tail behavior of the sample frequency distributions across the nine pairs of control-treatment watersheds, empirically estimated without the fitting of an assumed theoretical frequency distribution, ii) our ability to explain the differences in such tail behaviors by differences in physiography, climate, and harvesting regime between treatment watersheds, iii) the outcomes of this study align with existing probabilistic studies in the rain and snow environments, and iv) GRADEX (GRADient of EXtreme values) principles that lend further confidence in upper tail predictions, showing a physically defensible persistent gap between pre- and post-harvest FFCs, or convergence that will be shifted to higher return periods as sample size increases.

GRADEX principles are drawn from pluvial environments where, at high return periods, the FFC slope mirrors the rainfall frequency curve slope (Naghettini et al., 2012). In light of short sample sizes typically available in practice, GRADEX provides a means for corroborating the hypothesized effects on large return period events caused by forest harvesting or other forms of disturbance. Such methods are well understood in the wider hydrology literature (e.g., Brodie, 2020; Cœur and Lang, 2008; Guillot, 1993; Guillot & Duband, 1967; Mota et al., 2018; Naghettini et al., 2012).

Therefore, consistency in the tail behaviour of the peakflow frequency distributions are unlikely to be caused by sampling variability. As discussed earlier, it is the meta-analysis approach adopted in this study that builds confidence in the predicted effects of harvesting on events forming the upper tail of the sample peakflow frequency distributions.

4.5. *Implications on Larger Watersheds*

Although the experimental watersheds here are small, certain controls transcend scale: which controls influence hydrologic response regardless of watershed size, such that forest practices can be guided to prevent the exacerbation of peakflows in ROS environments? Previous studies have applied a similar probabilistic framework across a wide range of watershed sizes in rain- and snow-dominated environments, providing evidence of controls operating at multiple scales (Bradshaw et al., 2007; Green & Alila, 2012; Johnson & Alila, 2023; Kaluarachchi & Alila, 2026; Pearson-Atkins et al., 2026; Reynard et al., 2001). Similarly, the ROS environment will see a suite of controls that relate to larger scales.

Firstly, baseflow has an increasing influence on peakflow CV as watersheds get larger (Blöschl & Sivapalan, 1997). At elevated scales, and watersheds that have larger snow-transient zones, processes like meltwater and fog drip will play an increasing role in baseflow contributions, reducing pre-harvest peakflow variability. Physiographic heterogeneity and greater above- and below-ground storage impede runoff efficiency in larger watersheds, creating more opportunities for desynchronization. Climatic variability across larger scales, in antecedent wetness, snowpack, and storm characteristics, reinforces this effect. Consequently, this results in a much milder sloping FFC as watersheds get larger (Merz & Blöschl, 2009) demonstrating a greater level of sensitivity to changes in forest cover (Kaluarachchi & Alila, 2025), and in turn, larger changes in peakflow frequency will be experienced post-harvest.

Larger watersheds also accumulate runoff and sediment from headwater sub-watersheds, so the effects of forest practices there aggregate downstream and raise the probability of extreme events. Greater peakflow magnitude, frequency, and duration upstream drive cumulative downstream sedimentation, which alters fluvial geomorphology, reduces floodplain storage and channel capacity, and further exacerbates peakflows.

Watershed-level interpretations with increasing scale requires a mindset that goes beyond stand-level studies. With multiple physiographic (geographical context) and climatic (historical context) controls interacting stochastically with forest harvesting, a holistic understanding that accounts for upstream-downstream (or highland-lowland) causal links and considers the inherent multivariate intricate nature of snow-transient systems must be adopted. This will aid in the understanding of controls at varying scales, interpretation of cumulative effects downstream of headwater basins, and assist in sustainable forest management practices, policy (Bradshaw et al., 2009; Kaluarachchi & Alila, 2026), and engineering design (Beckers et al., 2002).

A caveat is that the snow-transient zone occupies a limited elevation band, so its share of watershed area depends on hypsometry; for basins extending well above or below this band the ROS-specific contribution may diminish with size. The synchronization controls invoked here, however, are not unique to ROS, the tendency toward milder frequency-curve slopes at larger scales operates across rain- and snow-dominated systems alike, so harvest sensitivity need not vanish even where the ROS fraction declines.

5. Conclusions

This study set out to advance the stochastic understanding of forest-harvesting effects on peakflows in the rain-on-snow environment by (i) applying a probabilistic, frequency-based framework; (ii) examining how harvesting-induced changes in water available for runoff and in runoff synchronization alter the mean and variability of peakflows; (iii) quantifying the consequential effects of these changes on the magnitude and frequency of peakflow events across all return periods; and (iv) assessing how watershed physiography and climate govern peakflow sensitivity to harvesting. Across the nine paired watersheds, harvesting and road effects on peakflows were more pronounced, but also more predictable, than much of the earlier deterministic literature implies. Whether infrequent peakflows (return periods greater than 10 years) are affected depends on the environmental controls: the effect was small at HJA1 and HJA3 but large at HJA6 and in the Coyote Creek and Fox Creek watersheds. In two Coyote Creek watersheds the effect on peakflow magnitude increased with event size, with no apparent no-effect threshold within the 17–50-year post-harvest records, and the frequency of the largest peakflows increased the most. Thus, large peakflows can increase in both magnitude and frequency, and can do so more than small and medium events.

The principal contribution is a synchronization/desynchronization framework that links peakflow response to the physiographic and climatic controls on the spatial and temporal variability of runoff generation and routing. Watersheds with large elevation ranges, wide aspect distributions, and elongated drainage networks tend to desynchronize runoff and so produce less flashy responses; because snow accumulation and ROS melt respond differently to harvesting across elevation bands, harvesting can further desynchronize generation and thereby offset part of its own tendency to raise the mean and variability of the frequency distribution. This single mechanism explains both the large response of subdued watersheds (HJA6, Coyote Creek, Fox Creek) and the muted response of steep ones (HJA1, HJA3, HJA10), and it clarifies why such scaling questions must be posed probabilistically: a purely deterministic, reductionist treatment admits contradictory outcomes that cannot be refuted by hypothesis testing. The framework also reframes fog interception: rather than treating it as an evapotranspiration- or canopy-interception-type water loss whose removal would only modestly raise peakflows, it is recast as a mechanism that suppresses the natural variability of the frequency distribution by offsetting early-season soil-moisture deficits and limiting sub-canopy snowpack development, so that its removal by harvesting can sharply increase variability and drive some of the largest frequency increases observed, as in the Fox Creek treatments. These inferences rest on isolating the treatment effect by pairing peakflows at equal frequency, on the wide range of watershed characteristics sampled (especially elevation range), and on the synchronization/desynchronization mechanism itself; together with Green and Alila (2012) in snow and Pham et al. (2025) in rain environments, this work illustrates that reliable physical understanding follows only when treatment effects are properly isolated, rarely done in nearly a century of paired-watershed research, which may help explain why harvesting effects on peakflows have so often appeared enigmatic and unpredictable (Alila et al., 2009).

These results carry practical implications. Increases in flood frequency translate directly into greater risk to stream crossings, levees, and other infrastructure, and large shifts in the peakflow frequency distribution alter the sediment and nutrient regimes that structure aquatic ecosystems. These are effects compounded by slow hydrological recovery, with no significant recovery detected in the first two decades after treatment (Schmidt & Potyondy, 2004). Several lines of work follow. Long-term deterministic simulation could extend the post-harvest records and corroborate or refute these findings, particularly the existence of a no-effect threshold return period (Birkinshaw et al., 2011; Reynard et al., 2001; Schnorbus & Alila, 2004, 2013). Additional long-term paired-watershed sites in North America and elsewhere could test the synchronization/desynchronization model across a wider range of hydroclimates, ideally by predicting the direction and magnitude of the harvesting response a priori from physiography, climate, and treatment regime and then verifying those predictions against the observed post-harvest frequency response; and, given heightened public concern, the effects of harvesting and roads in larger watersheds, where the spatial and temporal aggregation of processes should matter even more, warrant focused attention (Bradshaw et al., 2009). Under a changing climate, analyzing harvesting and road effects in a nonstationary setting could help reveal previously undetected peakflow sensitivities (e.g., Pearson-Atkins et al. (2026)), further guiding the future of hydrological-management policy.

Funding

This work was partially funded by the National Science and Engineering Research Council of Canada with Postgraduate Scholarships PGSD 663643 to W. Rong and Discovery Grant RGPIN 194388-11 to Y. Alila.

CRediT authorship contribution statement

WeiTao Nick Rong: Writing – review & editing, Writing – original draft, Visualization, Validation, Methodology, Formal analysis, Conceptualization. **Kyle S. Bishop:** Writing – review & editing, Visualization, Conceptualization. **Younes Alila:** Writing – review & editing, Supervision, Project administration, Conceptualization.

Declaration of competing interest

The authors declare that they have no known competing financial interests or personal relationships that could have appeared to influence the work reported in this paper.

Acknowledgements

We thank the three anonymous referees whose thoughtful feedback strengthened and greatly improved this paper.

Supplementary materials

Supplementary material associated with this article can be found, in the online version, at doi:10.1016/j.advwatres.2026.105432.

Data availability

Research Link Provided

Hydrological and GIS data from H.J. Andrews Experimental Forest LTER Data Bank (Reference data) (H.J. Andrews Experimental Forest LTER Data Bank)

References

Alexander, R.B., Boyer, E.W., Smith, R.A., Schwarz, G.E., Moore, R.B., 2007. The Role of Headwater Streams in Downstream Water Quality[1]. JAWRA Journal of the American Water Resources Association 43 (1), 41–59. https://doi.org/10.1111/j.1752-1688.2007.00005.x.

Alila, Y., Kuraś, P.K., Schnorbus, M., Hudson, R., 2009. Forests and floods: A new paradigm sheds light on age-old controversies. Water Resources Research 45 (8), 2008WR007207. https://doi.org/10.1029/2008WR007207.

Ashley, S.T., Ashley, W.S., 2008. Flood Fatalities in the United States. Journal of Applied Meteorology and Climatology 47 (3), 805–818. https://doi.org/10.1175/2007JAMC1611.1.

Azevedo, J., Morgan, D.L., 1974. Fog Precipitation in Coastal California Forests. Ecology 55 (5), 1135–1141. https://doi.org/10.2307/1940364.

Bathurst, J.C., Fahey, B., Iroumé, A., Jones, J., 2020. Forests and floods: Using field evidence to reconcile analysis methods. Hydrological Processes 34, 3295–3310. https://doi.org/10.1002/hyp.13802.

Beaudry, P., 1984. Effects of forest harvesting on snowmelt during rainfall in coastal British Columbia. University of British Columbia. https://doi.org/10.14288/1.0096022.

Beckers, J., Alila, Y., Mtiraoui, A., 2002. On the validity of the British Columbia Forest Practices Code guidelines for stream culvert discharge design. Canadian Journal of Forest Research 32 (4), 684–692. https://doi.org/10.1139/x02-010.

Berris, S.N., Harr, R.D., 1987. Comparative snow accumulation and melt during rainfall in forested and clear-cut plots in the Western Cascades of Oregon. Water Resources Research 23 (1), 135–142. https://doi.org/10.1029/WR023i001p00135.
Beschta, R.L., Pyles, M.R., Skaugset, A.E., Surfleet, C.G., 2000. Peakflow responses to forest practices in the western cascades of Oregon, USA. Journal of Hydrology 233 (1–4), 102–120. https://doi.org/10.1016/S0022-1694(00)00231-6.
Beven, K.J., 2000. Uniqueness of place and process representations in hydrological modelling. Hydrology and Earth System Sciences 4 (2), 203–213. https://doi.org/10.5194/hess-4-203-2000.
Birkinshaw, S.J., Bathurst, J.C., Iroumé, A., Palacios, H., 2011. The effect of forest cover on peak flow and sediment discharge—An integrated field and modelling study in central–southern Chile. Hydrological Processes 25 (8), 1284–1297. https://doi.org/10.1002/hyp.7900.
Blöschl, G., Sivapalan, M., 1997. Process controls on regional flood frequency: Coefficient of variation and basin scale. Water Resources Research 33 (12), 2967–2980. https://doi.org/10.1029/97wr00568.
Blum, A.G., Ferraro, P.J., Archfield, S.A., Ryberg, K.R., 2020. Causal Effect of Impervious Cover on Annual Flood Magnitude for the United States. Geophysical Research Letters 47 (5), e2019GL086480. https://doi.org/10.1029/2019GL086480.
Bradshaw, C.J.A., Brook, B.W., Peh, K.S.-H., Sodhi, N.S., 2009. Flooding Policy Makers with Evidence to Save Forests. AMBIO: A Journal of the Human Environment 38 (2), 125–126. https://doi.org/10.1579/0044-7447-38.2.125.
Bradshaw, C.J.A., Sodhi, N.S., Peh, K.S.-H., Brook, B.W., 2007. Global evidence that deforestation amplifies flood risk and severity in the developing world. Global Change Biology 13 (11), 2379–2395. https://doi.org/10.1111/j.1365-2486.2007.01446.x.
Brodie, I., 2020. Regional analysis of PROQ transforms for flood frequency estimation based on GRADEX principles. Australasian Journal of Water Resources 24 (2), 183–198. https://doi.org/10.1080/13241583.2020.1824368.
Brunengo, M. (2012). Where Is the Rain-on-Snow Zone in the West-Central Washington Cascades?: Monte Carlo Simulation of Large Storms in the Northwest. https://doi.org/10.15760/etd.689.
Christner, J., Harr, R.D., 1982. Peak stream flows from the transient snow zone, western Cascades, Oregon. In: Proceedings of the 50th Western Snow Conference, pp. 27–38.
Cœur, D., Lang, M., 2008. Use of documentary sources on past flood events for flood risk management and land planning. Comptes Rendus. Géoscience 340 (9–10), 644–650. https://doi.org/10.1016/j.crte.2008.03.001.
Comolatti, R., Hoel, E., 2022. Causal emergence is widespread across measures of causation.
Crampe, E.A., Segura, C., Jones, J.A., 2021. Fifty years of runoff response to conversion of old-growth forest to planted forest in the H. J. Andrews Forest, Oregon, USA. Hydrological Processes 35 (5). https://doi.org/10.1002/hyp.14168.
Eagleson, P.S., 1972. Dynamics of flood frequency. Water Resources Research 8 (4), 878–898. https://doi.org/10.1029/WR008i004p00878.
Flack, J.C., 2017. Coarse-graining as a downward causation mechanism. Philosophical Transactions of the Royal Society A: Mathematical, Physical and Engineering Sciences 375 (2109), 20160338. https://doi.org/10.1098/rsta.2016.0338.
Garvelmann, J., Pohl, S., Weiler, M., 2015. Spatio-temporal controls of snowmelt and runoff generation during rain-on-snow events in a mid-latitude mountain catchment. Hydrological Processes 29 (17), 3649–3664. https://doi.org/10.1002/hyp.10460.
Gillett, N.P., Cannon, A.J., Malinina, E., Schnorbus, M., Anslow, F., Sun, Q., Kirchmeier-Young, M., Zwiers, F., Seiler, C., Zhang, X., Flato, G., Wan, H., Li, G., Castellan, A., 2022. Human influence on the 2021 British Columbia floods. Weather and Climate Extremes 36, 100441. https://doi.org/10.1016/j.wace.2022.100441.
Green, K.C., Alila, Y., 2012. A paradigm shift in understanding and quantifying the effects of forest harvesting on floods in snow environments. Water Resources Research 48 (10), 2012WR012449. https://doi.org/10.1029/2012WR012449.
Guillot, P., 1993. The arguments of the gradex method: A logical support to assess extreme floods. IAHS-AISH 213, 287–298.
Guillot, P., Duband, D., 1967. Rapport I.7. La méthode du Gradex pour le calcul de la probabilité des crues à partir des pluies. In: Floods and Their Computation—Proceedings of the Leningrad Symposium. IASH, pp. 560–569.
Hammond, J., Anderson, B., Simeone, C., Brunner, M., Muñoz-Castro, E., Archfield, S., Magee, E., Armitage, R., 2025. Hydrological Whiplash: Highlighting the Need for Better Understanding and Quantification of Sub-Seasonal Hydrological Extreme Transitions. Hydrological Processes 39 (3), e70113. https://doi.org/10.1002/hyp.70113.
Hancock, C., Wlodarczyk, K., 2025. The role of wildfires and forest harvesting on geohazards and channel instability during the November 2021 atmospheric river in southwestern British Columbia, Canada. Earth Surface Processes and Landforms 50 (1), e6065. https://doi.org/10.1002/esp.6065.
Harr, R.D., 1980. Streamflow After Patch Logging in Small Drainages Within the Bull Run Municipal Watershed, Oregon. Research Paper PNW-268, USDA Forest Service, Pacific Northwest Forest and Range Experiment Station 19.
Harr, R.D., 1982. Fog Drip in the Bull Run Municipal Watershed, Oregon1. JAWRA Journal of the American Water Resources Association 18 (5), 785–789. https://doi.org/10.1111/j.1752-1688.1982.tb00073.x.
Harr, R.D., 1983. Potential for augmenting water yield through forest practices in western washington and western oregon. JAWRA Journal of the American Water Resources Association 19 (3), 383–393. https://doi.org/10.1111/j.1752-1688.1983.tb04595.x.
Harr, R.D., Coffin, B.A., 1992. Influence of timber harvest on rain-on-snow runoff: A mechanism for cumulative watershed effects. Interdisciplinary Approaches in Hydrology and Hydrogeology 455–469.
Harr, R.D., Coffin, B.A., Cundy, T.W., 1989. Effects of timber harvest on rain-on-snow run-off in the transient snow zone of the Washington cascades. Timber-Fish-Wildlife Project. http://andrewsforest.oregonstate.edu/sites/default/files/lter/pubs/pdf/pub4647.pdf.
Harr, R.D., Fredriksen, R.L., Rothacher, J., 1979. Changes in Streamflow Following Timber Harvest in Southwestern Oregon. USDA Forest Service Research Paper PNW 249, 22. -.
Harr, R.D., McCorison, F.M., 1979. Initial effects of clearcut logging on size and timing of peak flows in a small watershed in western Oregon. Water Resources Research 15 (1), 90–94. https://doi.org/10.1029/WR015i001p00090.
Hewlett, J.D., Hibbert, A.R., 1967. Factors affecting the response of small watersheds to precipitation in humid areas. Forest Hydrology 11, 275–290.
Hoel, E.P., Albantakis, L., Tononi, G., 2013. Quantifying causal emergence shows that macro can beat micro. Proceedings of the National Academy of Sciences 110 (49), 19790–19795. https://doi.org/10.1073/pnas.1314922110.
Ingraham, N.L., Matthews, R.A., 1995. The importance of fog-drip water to vegetation: Point Reyes Peninsula, California. Journal of Hydrology 164 (1–4), 269–285. https://doi.org/10.1016/0022-1694(94)02538-M.
Ingwersen, J.B., 1985. Fog Drip, Water Yield, and Timber Harvesting in the Bull Run Municipal Watershed, Oregon1. JAWRA Journal of the American Water Resources Association 21 (3), 469–473. https://doi.org/10.1111/j.1752-1688.1985.tb00158.x.
Isaac, L.A., 1946. Fog drip and rain interception in coastal forests. US Department of Agriculture Forest Service Research Note 34, 15–16.
Jennings, K., Jones, J.A., 2015. Precipitation-snowmelt timing and snowmelt augmentation of large peak flow events, western Cascades, Oregon: PRECIPITATION-SNOWMELT TIMING AND PEAK FLOWS, OREGON. Water Resources Research 51 (9), 7649–7661. https://doi.org/10.1002/2014WR016877.
Johnson, D.H., 1999. The Insignificance of Statistical Significance Testing. The Journal of Wildlife Management 63 (3), 763. https://doi.org/10.2307/3802789.
Johnson, R.S.H., Alila, Y., 2023. Nonstationary stochastic paired watershed approach: Investigating forest harvesting effects on floods in two large, nested, and snow-dominated watersheds in British Columbia, Canada. Journal of Hydrology 625, 129970. https://doi.org/10.1016/j.jhydrol.2023.129970.
Jones, J.A., 2000. Hydrologic processes and peak discharge response to forest removal, regrowth, and roads in 10 small experimental basins, Western Cascades, Oregon. Water Resources Research 36 (9), 2621–2642. https://doi.org/10.1029/2000WR900105.
Jones, J.A., Grant, G.E., 1996. Peak Flow Responses to Clear-Cutting and Roads in Small and Large Basins, Western Cascades, Oregon. Water Resources Research 32 (4), 959–974. https://doi.org/10.1029/95WR03493.
Kaluarachchi, S., Alila, Y., 2025. Managing extremes in the Anthropocene: A causal, stochastic physics approach. Frontiers in Environmental Science 13, 1643416. https://doi.org/10.3389/fenvs.2025.1643416.
Kaluarachchi, S., Alila, Y., 2026. Why forests can mitigate floods of all sizes: Evaluating the scientific basis for forest-based flood mitigation. Ambio. https://doi.org/10.1007/s13280-026-02346-6.
Katz, R.W., 1993. Towards a statistical paradigm for climate change. Climate Research 2, 167–175. https://doi.org/10.3354/cr002167.
Katz, R.W., Brown, B.G., 1992. Extreme events in a changing climate: Variability is more important than averages. Climatic Change 21 (3), 289–302. https://doi.org/10.1007/bf00139728.
Klemeš, V., 1978. Physically Based Stochastic Hydrologic Analysis. In: Advances in Hydroscience, 11. Elsevier, pp. 285–356. https://doi.org/10.1016/B978-0-12-021811-0.50010-3.
Kumar, N., Poonia, V., Gupta, B.B., Goyal, M.K., 2021. A novel framework for risk assessment and resilience of critical infrastructure towards climate change. Technological Forecasting and Social Change 165, 120532. https://doi.org/10.1016/j.techfore.2020.120532.
Langbein, W.B., 1949. Annual floods and the partial-duration flood series. Transactions, American Geophysical Union 30 (6), 879. https://doi.org/10.1029/TR030i006p00879.
Lewis, J., Reid, L.M., Thomas, R.B., 2010. Comment on "Forest and floods: A new paradigm sheds light on age-old controversies" by Younes Alila et al. Water Resources Research 46 (5), W05801. https://doi.org/10.1029/2009WR008766.
Lundberg, A., Calder, I., Harding, R., 1998. Evaporation of intercepted snow: Measurement and modelling. Journal of Hydrology 206 (3), 151–163. https://doi.org/10.1016/S0022-1694(97)00016-4.
Merz, R., Blöschl, G., 2009. Process controls on the statistical flood moments - a data based analysis. Hydrological Processes 23 (5), 675–696. https://doi.org/10.1002/hyp.7168.
Mota, T., Naghettini, M., Fernandes, W., Silva, F., 2018. Combination of the SCS-CN and the GRADEX models to maximum flow estimation. RBRH 23 (0). https://doi.org/10.1590/2318-0331.231820170123.
Naghettini, M., Gontijo, N.T., Portela, M.M., 2012. Investigation on the properties of the relationship between rare and extreme rainfall and flood volumes, under some distributional restrictions. Stochastic Environmental Research and Risk Assessment 26 (6), 859–872. https://doi.org/10.1007/s00477-011-0530-4.
Naman, S.M., Pitman, K.J., Cunningham, D.S., Potapova, A., Chartrand, S.M., Sloat, M. R., Moore, J.W., 2024. Forestry impacts on stream flows and temperatures: A quantitative synthesis of paired catchment studies across the Pacific salmon range. Ecological Solutions and Evidence 5 (2), e12328. https://doi.org/10.1002/2688-8319.12328.
Pearson-Atkins, S., Yu, X.J., Alila, Y., 2026. Nonstationary frequency pairing reveals a highly sensitive peak flow regime to harvesting across a wide range of return periods. Forest Ecology and Management 617. https://doi.org/10.1016/j.foreco.2026.123895.

Perry, T.D., Jones, J.A., 2017. Summer streamflow deficits from regenerating Douglas-fir forest in the Pacific Northwest, USA. Ecohydrology 10 (2), e1790. https://doi.org/10.1002/eco.1790.

Pham, H.C., Alila, Y., 2024. Science of forests and floods: The quantum leap forward needed, literally and metaphorically. Science of The Total Environment 912, 169646. https://doi.org/10.1016/j.scitotenv.2023.169646.

Pham, H.C., Alila, Y., Caldwell, P.V., 2025. Stochastic framework reveals the controls of forest treatment – peakflow causal relations in rain environment. Journal of Hydrology, 133704. https://doi.org/10.1016/j.jhydrol.2025.133704.

Climate Group, PRISM, 2004. PRISM Gridded Climate Data. Oregon State University.

Reynard, N.S., Prudhomme, C., Crooks, S.M., 2001. The Flood Characteristics of Large U.K. Rivers: Potential Effects of Changing Climate and Land Use. Climatic Change 48 (2/3), 343–359. https://doi.org/10.1023/A:1010735726818.

Robinson, M., 1986. Changes in catchment runoff following drainage and afforestation. Journal of Hydrology 86 (1–2), 71–84. https://doi.org/10.1016/0022-1694(86)90007-7.

Robinson, J.S., Sivapalan, M., 1997. Temporal scales and hydrological regimes: Implications for flood frequency scaling. Water Resources Research 33 (12), 2981–2999. https://doi.org/10.1029/97WR01964.

Rosas, F.E., Mediano, P.A.M., Jensen, H.J., Seth, A.K., Barrett, A.B., Carhart-Harris, R.L., Bor, D., 2020. Reconciling emergences: An information-theoretic approach to identify causal emergence in multivariate data. PLOS Computational Biology 16 (12), e1008289. https://doi.org/10.1371/journal.pcbi.1008289.

Rosentrater, L.D., 1997. The thermal climate of the H.J. Andrews Experimental Forest, Oregon. University of Oregon.

Salas, J.D., Obeysekera, J., 2014. Revisiting the Concepts of Return Period and Risk for Nonstationary Hydrologic Extreme Events. Journal of Hydrologic Engineering 19 (3), 554–568. https://doi.org/10.1061/(asce)he.1943-5584.0000820.

Schmidt, L.J., Potyondy, J.P., 2004. Quantifying channel maintenance instream flows: An approach for gravel-bed streams in the Western United States. USDA Forest Service - General Technical Report RMRS-GTR, 128 RMRS-GTR, pp. 1–36. http://www.scopus.com/inward/record.url?eid=2-s2.0-34247327374&partnerID=40&md5=1799e6ecddd6a152c448c7eff4f146bd.

Schnorbus, M., Alila, Y., 2004. Forest harvesting impacts on the peak flow regime in the Columbia Mountains of southeastern British Columbia: An investigation using long-term numerical modeling. Water Resources Research 40 (5), 2003WR002918. https://doi.org/10.1029/2003WR002918.

Schnorbus, M., Alila, Y., 2013. Peak flow regime changes following forest harvesting in a snow-dominated basin: Effects of harvest area, elevation, and channel connectivity. Water Resources Research 49 (1), 517–535. https://doi.org/10.1029/2012WR011901.

Sicart, J.E., Essery, R.L.H., Pomeroy, J.W., Hardy, J., Link, T., Marks, D., 2004. A Sensitivity Study of Daytime Net Radiation during Snowmelt to Forest Canopy and Atmospheric Conditions. Journal of Hydrometeorology 5 (5), 774–784. https://doi.org/10.1175/1525-7541(2004)005%3C0774:assodn%3E2.0.co;2.

Sivakumar, B., 2017. Chaos in Hydrology—Bridging Determinism and Stochasticity. Springer, Netherlands. https://doi.org/10.1007/978-90-481-2552-4.

Sivapalan, M., Beven, K., Wood, E.F., 1987. On hydrologic similarity: 2. A scaled model of storm runoff production. Water Resources Research 23 (12), 2266–2278. https://doi.org/10.1029/WR023i012p02266.

Stedinger, J.R., Vogel, R.M., Foufoula-Georgiou, E., 1993. Frequency analysis of extreme events. In: Maidment, D.R. (Ed.), Handbook of Hydrology. McGraw-Hill, 18.1-18.66.

Storck, P., Lettenmaier, D.P., Bolton, S.M., 2002. Measurement of snow interception and canopy effects on snow accumulation and melt in a mountainous maritime climate, Oregon, United States. Water Resources Research 38 (11). https://doi.org/10.1029/2002WR001281.

Talbot, C.J., Bennett, E.M., Cassell, K., Hanes, D.M., Minor, E.C., Paerl, H., Raymond, P.A., Vargas, R., Vidon, P.G., Wollheim, W., Xenopoulos, M.A., 2018. The impact of flooding on aquatic ecosystem services. Biogeochemistry 141 (3), 439–461. https://doi.org/10.1007/s10533-018-0449-7.

Thomas, R.B., 1990. Problems in determining the return of a watershed to pretreatment conditions: Techniques applied to a study at Caspar Creek, California. Water Resources Research 26 (9), 2079–2087. https://doi.org/10.1029/wr026i009p02079.

Thomas, R.B., Megahan, W.F., 1998. Peak flow responses to clear-cutting and roads in small and large basins, Western Cascades, Oregon: A second opinion. Water Resources Research 34 (12), 3393–3403. https://doi.org/10.1029/98WR02500.

USDA-NRCS, 2007. Stream Hydrology. In: Bernard, J.M., Fripp, J., Robinson, K. (Eds.), *Part 654 Stream Restoration Design National Engineering Handbook* (Chapter 5). US Department of Agriculture, Natural Resources Conservation Service.

Wang, T., Hamann, A., Spittlehouse, D.L., Murdock, T.Q., 2012. ClimateWNA-high-resolution spatial climate data for western North America. Journal of Applied Meteorology and Climatology 51 (1), 16–29. https://doi.org/10.1175/JAMC-D-11-043.1.

Winkler, R., Boon, S., 2015. Revised Snow Recovery Estimates for Pine-Dominated Forests in Interior British Columbia. BC Min. For. Lands. Nat. Res. Oper., Research Extension Note 116 (September), 1–11.

Yevjevich, V., 1974. Determinism and stochasticity in hydrology. Journal of Hydrology 22 (3–4), 225–238. https://doi.org/10.1016/0022-1694(74)90078-X.